5G SLOT ANTENNA DESIGN WITH MACHINE LEARNING

by

ONUR ELÇİN

Submitted to the Graduate School of Engineering and Natural Sciences

in partial fulfillment of

the requirement for the degree of Master of Science

Sabancı University

June 2022

ABSTRACT

5G SLOT ANTENNA DESIGN WITH MACHINE LEARNING

ONUR ELÇİN

Electronics Engineering, M. Sc. Thesis, July 2022

Thesis Supervisor: Prof. İbrahim Tekin

Keywords: 5G, Slot Antenna, Machine Learning, Deep Learning

5G technology is promising to be the future technology due to its higher data output, lower latency, and higher channel capacity. Many transceiver structures are designed for 5G and antennae play a crucial role in these structures with their gain, bandwidth, and directional properties. To satisfy the needs of the system, RF engineers use tools such as HFSS, AWR, and CST to design optimum antennas. These tools can simulate the real behavior of antennae at the cost of time and hardware memory. To solve the computation cost issue, this thesis focused on using machine learning tools to do antenna design. First, a slot antenna topology was chosen based on the 5G antenna and designed using HFSS and traditional optimization methods. The parameters of the chosen topology were swept to create a dataset for machine learning. This dataset was used for predicting realized gain and s-parameters. To find the optimum design, input parameters in the datasets were interchanged with output parameters to locate the best lengths. These lengths were swept with machine learning and deep learning tools to exhaustively search for an improved design. As a result of this multi-step process, a better-performing antenna was designed in a shorter time and with less computation cost.

ÖZET

MAKİNE ÖĞRENMESİ İLE BOŞLUKLU 5G ANTEN TASARIMI

ONUR ELÇİN

Elektronik Mühendisliği, Yüksek Lisans Tezi, Haziran 2022

Tez Danışmanı: Prof. İbrahim Tekin

Anahtar Kelimeler: 5G, Boşluklu Anten, Makine Öğrenmesi, Derin Öğrenme,

5G teknolojisi yüksek veri kapasitesi, düşük gecikme ve arttırılmış kanal kapasitesi ile geleceğin teknolojisi olma yolundadır. Bu teknoloji ile uyumlu alıcı-verici sistemleri tasarlanmaktadır ve bu sistemlerde kazanç, bant genişliği ve yönlülük özellikleri ile antenler önemli bir rol oynamaktadır. Teknolojinin gereksinimlerini karşılamak için HFSS, AWR ve CST gibi tasarım araçları mühendisler tarafından sıkça kullanılmaktadır. Her ne kadar bu simülasyon araçları anten özelliklerini gerçeğe çok yakın bir şekilde tahmin edebilse bile ciddi miktarlarda zaman ve donanım kaynakları kullanırlar. Bu sorunların üstesinden gelebilmek için makine öğrenme ile anten tasarımı yapmak bu tezin konusu olmuştur. Tezin ilk aşaması olarak boşluklu bir anten yapısı seçilmiştir ve klasik tasarım metotları ile HFSS ile bir tasarım ortaya konulmuştur. Bu tasarımında kritik rol oynayan uzunluk parametreleri değiştirilerek farklı tasarımlar oluşturuldu ve performans parametreleri kaydedilerek bir veri tabanı yaratıldı. Bu veri tabanı makine öğrenmesi ile antenlerin kazançları ve yansıma katsayılarını belirlemek için kullanılmıştır. En uygun tasarımı bulabilmek için girdi ve çıktı parametreleri yer değiştirilerek uzunluk bilgileri güncellenmiştir. Bu güncellemeden sonra bulunan uzunluklar makine öğrenmesi ve derin öğrenme algoritmaları ile bir daha taranmıştır. Birkaç adım içeren bu tasarım sürecinin sonunda daha iyi performansa sahip bir anten daha hızlı ve daha az donanım gereksinimi ile tasarlanmıştır.

ACKNOWLEDGEMENTS

I would like to thank my professor İbrahim Tekin, who was the instructor of many RF courses I have taken in the past. Without your teachings and passion, I do not know if I would be the engineer you see today. Consider this thank you not only for the enormous contribution you made during my thesis studies but also for the inspiration you gave over the years of my undergraduate education. I wish you to never lose your passion not only for electronics but also for teaching.

It was a great pleasure to get to know Prof. Hüsnü Yenigün during my thesis studies. I have heard his name only a few times but never had the chance to meet him in person. Thanks to this project, I was able to be acquainted with you, and thank you for all the support during this period.

It is also my wish to thank Amir Mohsen Ahmadi for his help. I still remember how you tried to follow every meeting we did even if you had a lot of other work to do as a graduate student like me. I appreciate your support and wish you success in your studies.

DEDICATIONS

My family have always supported me, and it is a fact that they are the ones who made me who I am, but I must give a special thanks to my mother and father. They were always there to cheer me up when I was frustrated and stuck on a problem. They always showed guidance during both my master's education and work life. This thesis would not be here if it wasn't for them.

It would be a shame if I did not mention my former manager, Dr. Ferdi Tekçe. During this whole graduate education, he was the one who pushed me to pursue both a master's degree and the electronics industry at the same time. Without his support and inspiration, I had already given up one or another. Thank you for all your care and help Mr. Tekçe.

TABLE OF CONTENTS

LIST OF TABLES AND FIGURES

List of Figures

List of Tables

LIST OF SYMBOLS AND ABBREVIATIONS

1G	: 1st Generation
2G	: 2nd Generation
3D	: 3 Dimensional
3G	: 3rd Generation
4G	: 4th Generation
5G	: 5th Generation
5G NR	: 5G New Radio
AWR	: Applied Wave Research
CST	: Computer Simulation Technology
dB	: decibel
dBi	: decibel relative to isotropic antenna
DL	: Deep Learning
DUT	: Device Under Test
FEM	: Finite Element Method
G_r	: Power received in the receiver antenna
G_t	: Power transmitted from transmitter antenna
GHz	: Gigahertz
GB	: Gigabyte
GND	: Ground
GPS	: Global Positioning System
HFSS	: High-Frequency Structure Simulator
KNN	: K Nearest Neighbors
LTE	: Long-Term Evolution
MAE	: Mean Absolute Error
MHz	: Megahertz
ML	: Machine Learning
NoFDMA	: Non-Orthogonal Frequency Division Multiple Access
OFDMA	: Orthogonal Frequency Division Multiple Access
P_r	: Gain of receiver antenna
P_t	: Gain of the transmitter antenna
RAM	: Random Access Memory

RAN : Radio Access Network

RG : Realized Gain

S11 : Ratio of reflected power to incident power at port 1

SNR : Signal to Noise Ratio

StD : Standard Deviation

SUNUM : Sabancı University Nanotechnology Research Center

UE : User Equipment

INTRODUCTION

The antenna is a crucial part of transceiver systems, and this section will briefly explain the main problems encountered during the design process. Then a solution to this problem will be proposed with the usage of machine learning. The rest of this chapter is left to the explanation of the thesis roadmap to give a clear understanding of the steps taken.

1.1. Problem Definition

Antenna design starts with the determination of theoretical lengths. To verify the lengths, simulation tools such as HFSS, CST and AWR are used. These tools can include many parasitic effects that are not included in the theory. Due to these effects, the initial design generally does not hold up to the expectations. To overcome this situation, lengths in the design are swept to find optimum values. Due to the nature of trial and error, it is hard to define how long it will take to complete the optimization process.

In a study, it was shown that simulation of a 4x4 array takes around 6 min with 0.7 GB RAM usage, but the same setup with a 16 x 16 array takes 8 hours with 11.6 GB RAM usage [1]. The time it takes for each simulation can differ from seconds to hours, increasing exponentially as the sizes increase. The designer is in a spot where he/she must do a trade-off between accuracy and speed. Even though there are methods to speed up the process, such as symmetry and boundary assumptions, these assumptions come with their own accuracy problems. The time and resource problems have become even more important for 5G technologies due to the requirement of custom solutions for clients. To fulfill every need, the design process must be sped up considerably.

1.2. Proposed Solution

This thesis proposes to decrease the time and hardware required for antenna design by using machine learning tools. Machine learning algorithms extract a model from a dataset to predict a new data point. This method can be used to determine the performance parameters of an antenna without the need for simulation software. After a model is trained, it only requires input parameters to make a prediction.

Another advantageous part of machine learning is its ability to discover hidden patterns. Instead of predicting the performance parameters of an antenna, the thesis moves the limits one step further by predicting the length parameters. This is done by interchanging input and output variables to predict a length at a specific performance point. This approach enables the designer to test a configuration that was not in the scope of initial parameters, thus facilitating the design process even more. Using performance parameters as inputs also lets the designer customize the antenna as the new requirements are added, thus improving the flexibility of the whole process.

1.3. Thesis Organization

After a brief description of the problem and proposed solution in the first chapter, the thesis will continue with key background information about the topic. Topics covered will be 5G technology, software used for antenna design, and work done related to machine learning in antenna design. Due to the interdisciplinary structure of this thesis, it is aimed at giving a clear understanding of key concepts from both disciplines.

The third chapter will be about the design of the proposed antenna. Traditional design methods will be covered in this section and their effect on the antenna performance will be displayed. The main purpose of this section is to show the steps of the design process and the effort needed to achieve a well-performing antenna.

After the completion of the initial antenna design, the machine learning part of the thesis will be included. The beginning of the fourth chapter will explain how an antenna design problem is converted into a machine learning problem and continue with dataset

generation and features of the dataset. Then suitable algorithms for the proposed solution will be explained and their performance will be evaluated with cross-validation. The best-performing algorithm will be chosen as the basis for the next steps. Finally, the chapter will be concluded with a novel iterative way of predicting length parameters by interchanging input and output parameters. A score metric is also added to make an alternative way of comparing results. An extra step of exhaustive sweep will be done to improve the design even further.

A subset of machine learning, deep learning, will be discussed in the fifth chapter and neural networks will be used for antenna design like machine learning. Designs created by deep learning and machine learning algorithms will be compared. To extend the application of the learning tools, two separate designs will be made for 25 GHz and 31 GHz with both machine learning and deep learning. Then the thesis will be concluded with a comparison of the results and a discussion about achievements.

BACKGROUND

This chapter of the thesis will cover the key background information required. A brief introduction to 5G will be told to explain the reasoning behind the choice over other technologies such as 3G and 4G. A summary of antenna design tools will be given to discuss their operating mechanism and to derive advantages and disadvantages. The chapter will be concluded with a review of other machine learning applications in the antenna design area to understand the state of the art.

2.1. Importance and Place of 5G

To understand the drive behind the 5G technology, it is important to realize the trend over the years. When the data rate of technologies used in the last 40 years is compared, an approximately 10-fold increase in data rate is observed every decade [2]. To satisfy the data rate requirement of user equipment (UE), millimeter wave frequency became the obvious choice and initiated the foundation of 5G technology.

A similar argument can be made for channel capacity. With an increasing number of UE, the number of participants in each communication channel also increases. Even though there are methods such as OFDMA (Orthogonal Frequency Division Multiple Access) to increase the channel capacity by distributing channel resources orthogonally, they are still limited by the total resources of the channel [3]. An improved version of OFDMA, NoFDMA (Non-orthogonal Frequency Division Multiple Access), is promising to increase the channel capacity while keeping the user's performance the same, but it is questionable whether overloading of the channel (including more users than the channel limit) can be scaled up as the demand increases [4]. 5G technology provides a simple

solution by introducing a higher capacity channel with higher operating frequencies and bandwidths.

Even though higher data output and channel capacity are the most advertised properties of 5G technologies, low latency should not be forgotten. Low latency is even more important for mission-critical communications such as telediagnosis, telesurgery, virtual reality, and augmented reality. Today's standard 4G RAN (Radio Access Network) limits these applications due to its old structure. 5G technologies can operate shorter time windows, thus it is possible for this technology to lower latency with smaller sized packets, new coding, and modulation schemes [5]. The benefits of lower latency will be more visible as concepts such as virtual reality continue to become a part of the daily routine with the help of 5G.

The higher data rate, channel capacity, and lower latency are the driving features of 5G technology and the reason behind these features can be summarized as the usage of millimeter waves [6]. Although the benefit of using a higher frequency is non-negligible, new challenges arise with this frequency. As seen in Frii's Transmission Equation given below, received signal power decreases proportionally to the square of decreased wavelength λ [7]:

$$P_r = G_t G_r P_t \left(\frac{\lambda}{4\pi r}\right)^2 \qquad 2.1$$

From LTE frequencies to microwave frequencies, there is at least an extra 20 dB extra power loss expected for 5G applications theoretically. For some low signal-to-noise ratio (SNR) applications like radar and satellite communication, such conditions directly invalidate the application itself. It is important to note that this is the theoretical extra path loss. There can be other obstacles in the medium of the wave traveling, thus decreasing the signal power level even more. A recent study shows that materials become harder to penetrate as the frequency increases from the low GHz region to 10 GHz [8]. The degree of loss depends on the material type and thickness. Nevertheless, millimeter wave signals have lower penetration compared to larger wavelengths [9] .

Both penetration issues and higher path loss decrease the power level of 5G signals. To overcome these issues, many RF transceivers are forced to maximize their gains and minimize system losses. Antennae are also subject to this restriction. One way to improve performance is to use an array formation. With antenna arrays, higher directivity leads to higher gains, but it requires proper feeding and placement. Some studies focus on antenna and array topologies to improve gain and bandwidth properties. One recent study uses defected ground structures and slots to improve the performance of the radiating element and the whole structure is inkjet-printed to facilitate the production [10]. Another work focuses on placing two different antenna array formations with different radiating elements to improve coverage [11]. Many other examples can be given and all of them share a common point. To establish the basis of 5G, custom antennae and array solutions are required, and this is only possible with an accelerated design process.

2.2. Tools Used for Antenna Design

Whether it is a GPS antenna or a mobile antenna for 5G, every antenna design starts with the theoretical determination of initial lengths. This can be done using formulas if it is a well-formulated topology, or an existing design can be adapted by changing radiating element sizes concerning operating frequency. It is hard to determine the exact behavior of the first design, so simulation software such as HFSS, CST, and AWR is used to simulate the performance and do optimization. The working principle explained will be about HFSS, but other software shares a similar principle.

HFSS uses FEM (Finite Element Method) method to divide a 3D structure into many smaller parts. These parts are finite elements used for calculating the electric fields based on boundary conditions [12]. After the first calculation of the electric fields, the error metric is controlled and if it is above the user-defined limit, a higher mesh is applied to divide the structure into even smaller parts [13]. Electric fields are calculated one more time and the process is repeated until the error metric is lower than the limit. When the error residual is below the limit, the software continues to calculate performance parameters of the design at a given frequency. A flow chart of the FEM steps can be seen in Figure 1.

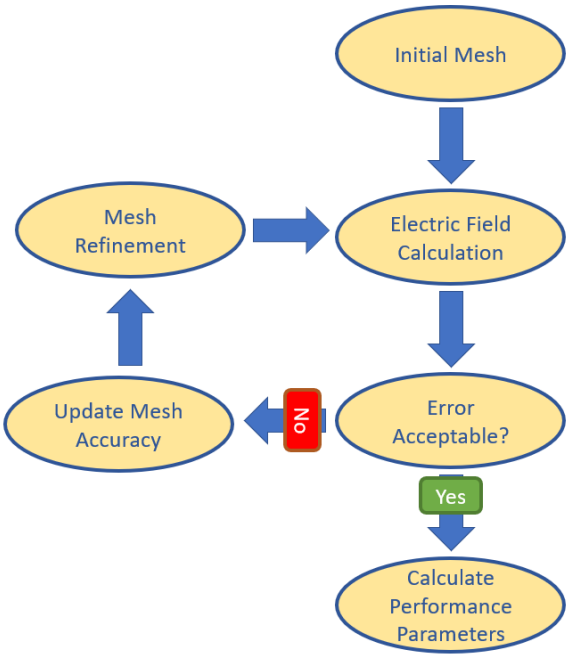

Figure 1: HFSS FEM steps

With FEM, HFSS can give accurate results but there is always a tradeoff between accuracy and the computation time. The main reasons behind the computation cost can be listed as:

- Strict accuracy limitation
    - A higher accuracy results with a large mesh, which increases the computation time.
- High frequency of operation
    - Shorter wavelengths require a denser mesh to include all electromagnetic effects.
- Broadband applications
    - Each solution must be prepared for each frequency of interest, so the complexity problem scales with bandwidth.

In the case of 5G applications, a shorter wavelength directly increases the mesh density. Even designs with low fractional bandwidth can have bandwidths in the range of GHz. The only trade-off mechanism that is left is accuracy, which must be kept as high as possible. Even though HFSS and many other tools are preferred for 5G antenna design, their computational cost remains a debated topic.

2.3. Usage of Machine Learning with Antenna Design

Computation cost of the electromagnetic simulation tools remains a major issue. The nature of the design process is like a trial-and-error method. To optimize the design, the designer must sweep as many parameters as possible. The sweep set increases exponentially as the number of parameters and sweep range increases. The process becomes unfeasible very fast and the designer is forced to use intuition to guess the best way to optimize. Even though there are optimizers which use a cost function to test multiple designs, they are still bound by the computation resources required for each test.

An interesting method to solve this issue appeared as machine learning tools became more popular. These tools were able to extract a pattern from a dataset to make prediction for a new data point. Such models achieved great success in areas like image and voice recognition and did not take a lot of time to take part in antenna design. A study in 2020 showed that it is possible to do antenna matching with machine learning and the effect of each parameter on reflection coefficient is also analyzed [14]. Even though the research focused on tuning a single parameter, the results looked promising. Another recent study focused on reviewing the accuracy of well-known machine learning algorithms on chosen a set of antennas [15]. Results showed that in every design, machine learning algorithms were faster with reasonable accuracy. The findings of the paper were parallel with the expectations, but the evaluation of these tools with multioutput problems was not included. Usage of machine learning was not limited by the design of the radiating element. A recent research paper argued that it is possible to optimize cellular network deployment by reinforcement learning. The paper showed that conventional algorithms are prone to increase network size due to their high complexity and suggested a novel way to optimize cellular networks [16].

Many examples can be found in literature about antenna design and its benefits to the design process, but most of the arguments were centered on the speed aspect. Additionally, machine learning tools were used mostly as supplementary tools instead of the design tool itself. To do a design just using machine learning tools and its performance still requires extra research and time.

TRADITIONAL ANTENNA DESIGN

A 5G slot antenna will be designed for demonstrating steps taken and resources used during an antenna design process. In the beginning, the chapter will mention design steps and end goals. A discussion about the topology choice will be done and it will be followed by the design phase itself. This phase will consist of steps taken to optimize the results. Results will be displayed at the end of the chapter and a brief discussion about the performance and resources used will be shown.

3.1. Design Flow and Goals

The design phase starts with the establishment of the expected performance of the antenna. As the first step, the antenna must fulfill these conditions:

- The antenna operating frequency will be centered at 28 GHz and must have a bandwidth of 3 GHz. More specifically, the designed antenna will function in the n257 band, which has the highest number of 5G NR networks deployed around the globe [17].

- The designed antenna is expected to have around 5 dBi gain in a given bandwidth.

- The antenna must be directional and there should not be any major back lobe or side lobe. Any strong side/back lobe formation may cause interference problems with other parts of the transceiver.

- The topology chosen must be unique to a degree. Well-known topologies, such as patch antenna, inverted F-antenna, and Vivaldi antenna, are already formulated and modelled in the literature. There is not any advantage of creating machine learning models of these topologies.

- The topology chosen must be easy to parametrize. Shapes like spirals and irregular polygons require a lot of lengths and coordinate parameters. Such conditions increase the size of the model and limit the applicability of the model to other topologies with similar shape.

It is important to realize that the designed antenna does not have to be a slot antenna, but the properties of this topology, which will be told in the next part, are parallel with the requirements. When the topology choice is concluded, an initial design will be constructed, and features of the antenna will be adjusted according to the needs of the design at that point.

3.2. Topology Choice

Recent 5G antenna publications were analyzed and designs in line with the requirements of the thesis were chosen. A common trait of the designs is their slot base. Slot type is advantageous due to their flexibility over performance with both patch and slot tuning. Additionally, their shape can be well defined with parameters such as patch position/size and slot position/size. The best four candidates are shown in Figure 2 and each design has the following properties:

- Figure 2a is a T-slot type antenna for mobile terminals and specifically designed for array formations. Array formation has a center frequency of 28 GHz and bandwidth of 2 GHz approximately [18]. The array has a gain of 10 dB with 8 radiating elements, but the main lobe has a large circular radiation pattern with a coverage range of 360^{o}. A radiation in a single direction would be more advantageous.

- Another slot-based antenna is shown in Figure 2b. This topology used two different designs as a pair for both 4G and 5G systems. Ant-3 and Ant-4 operate at 28 GHz with a bandwidth of 1.5 GHz and have 10 dBi gain as an array [19]. The radiation pattern consists of two large side lobes instead of one and radiating elements are also made of sub elements to increase the gain. The performance of the antenna is dependent on a large floating patch which makes the whole design unnecessarily large.

- A similar topology is shown in Figure 2c. Unlike the previous design, the radiating elements are placed on opposite sides and fed with two separate feedlines. The design has a bandwidth of 2 GHz with a center frequency of 27.5 GHz and outputs 9.5 dBi gain as an array formation [20]. Like previous topology given in Figure 2c, there are multiple slots in various coordinates which is not suitable for parametrization.

- Topology in Figure 2d has a couple of distinct features. It is straightly designed as a single element and has broadband characteristics. The proposed antenna has a bandwidth of 20 GHz centered at 30 GHz and a varying gain of 2 – 4 dBi over the bandwidth [21]. This antenna also suffers from a back lobe, but the large bandwidth leaves designers room for trade off and single element design is more flexible, unlike the strict positioning requirements of arrays. Due to the potential, this topology was chosen as the basis of this paper.

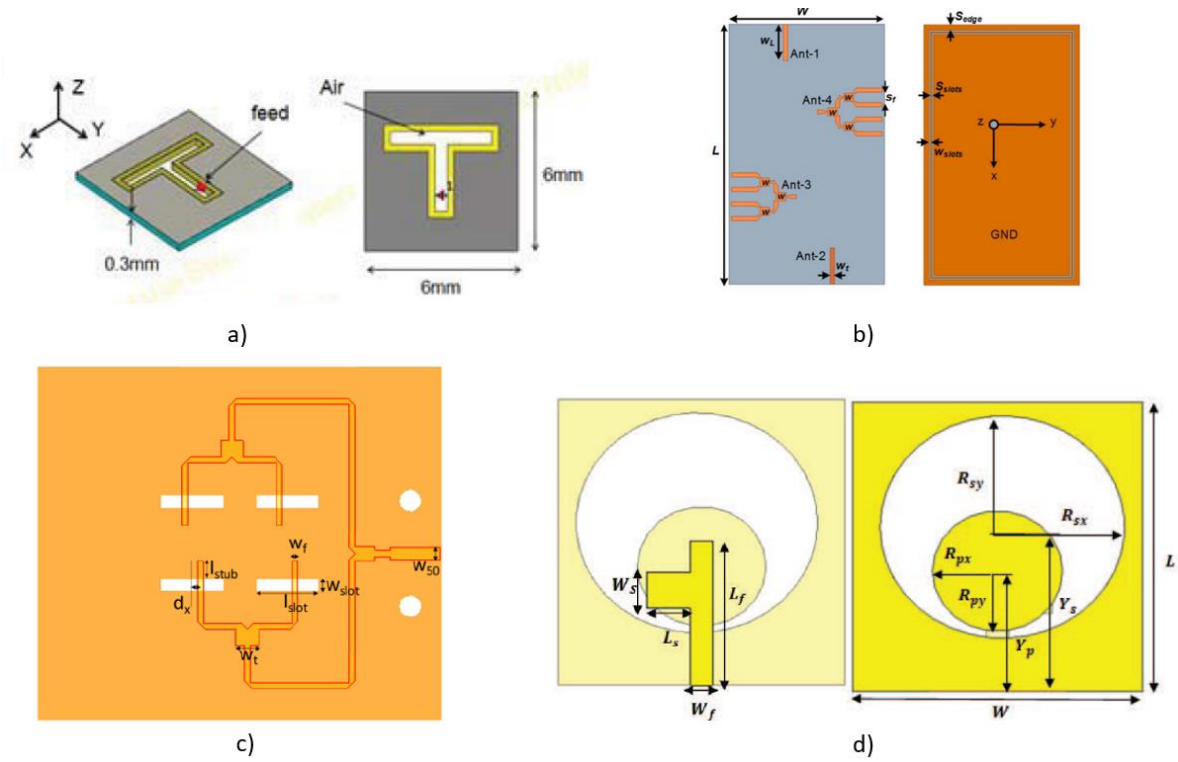

Figure 2: Best candidates for desired topology: (a) T-type slot antenna, (b) 4G and 5G combined slot, (c) opposite placed slot array and (d) broadband circular slot antenna

Lower gain and the existence of the back lobe are the main flaws of the chosen topology. These flaws will be the main topic of the design phase and various methods will be tested to improve those aspects.

3.3. Design Phase

To improve the bandwidth and prevent back lobe radiation, size of feed, patch and slot were tested with different values, but back lobe radiation remained comparable to the main lobe as shown in Figure 3.

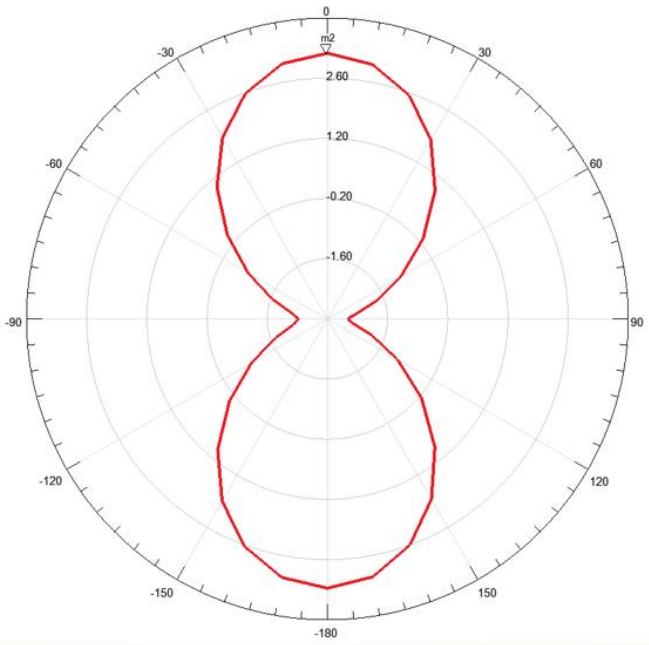

Figure 3: Front and back lobe radiation of initial design at 28 GHz

To completely negate the back lobe, addition of an extra layer was decided. The reasoning comes from image theory. Image theory states that electric fields created by charges next to conductive surfaces experiences mirroring effect. This effect can be realized as the existence of a new charge as it is mirrored over the conductive surface [22]. The idea is to reflect lobe radiation to the front side by careful placement of the metal surface. With addition of an extra layer, a stack-up in Figure 4 was created. The reflector ground plane removed the back lobe as shown in Figure 5 and the broadband characteristic is also removed as shown in Figure 6.

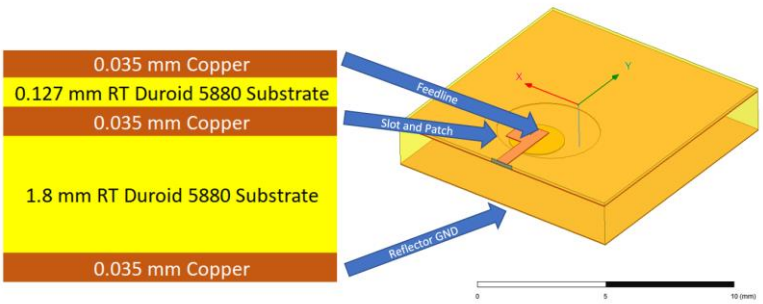

Figure 4: Stack-up and top view of floating GND added design

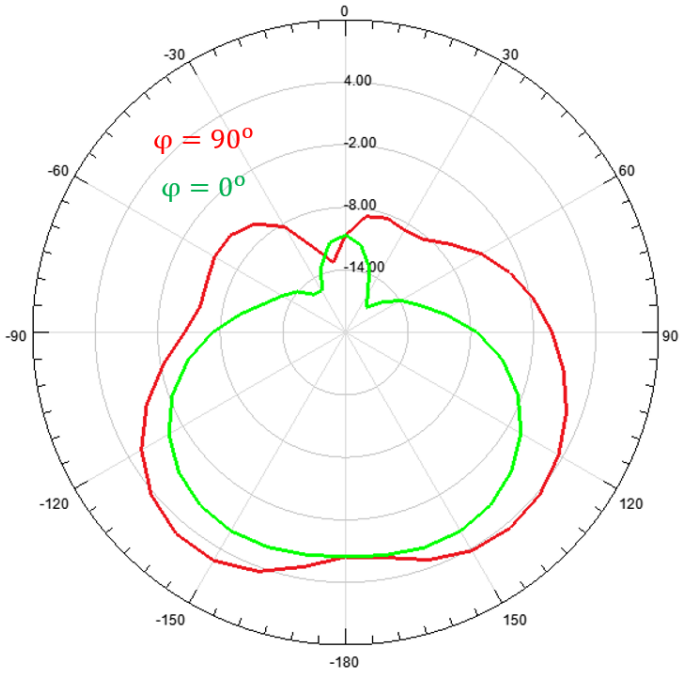

Figure 5: Radiation pattern of floating GND added design at 28 GHz and φ= 0° / 90°

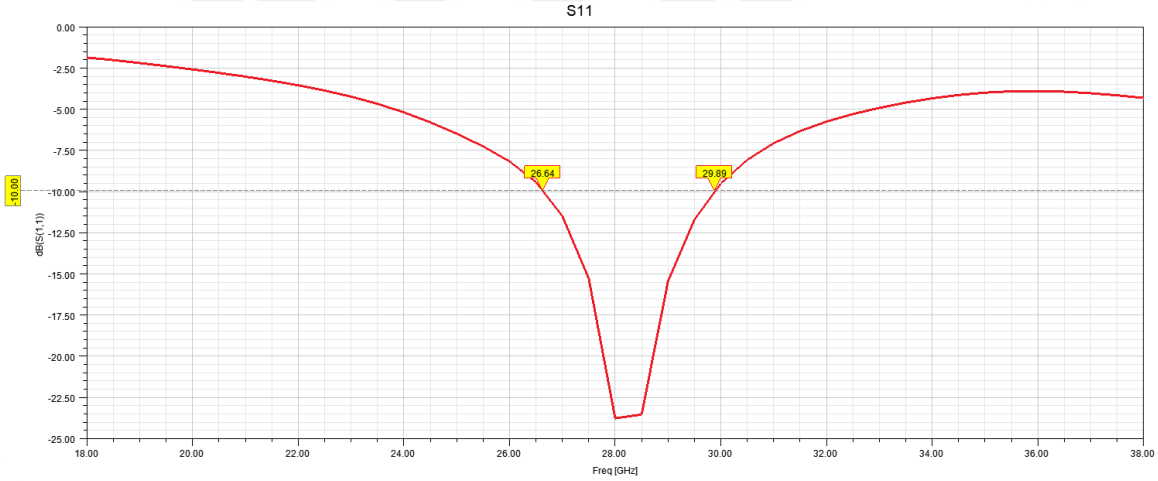

Figure 6: S11 of reflector GND added design

Even though the main problems of the initial design were solved, addition of a floating GND had other issues:

- The design still did not have a major main lobe and the existence of two sides lobes causes signal transmission in an unwanted direction.

- These performances are achieved with a 1.8 mm RT Duroid 5880 substrate which is not a standard substrate size and the design is not suitable for edge feed coaxial connector.

The design is impractical for fabrication, so a more realistic design can be seen in Figure 7. The floating ground patch and substrate were kept shorter to leave enough headroom for the connector. Additionally, screw holes were added for inclusion of parasitic effects. The stub used for matching was also removed to simplify the design. Parameters that are crucial for performance are shown in Figure 8 and their values are displayed in Table 1. These parameters were measured with respect to connector headroom to keep the lengths consistent with the initial topology.

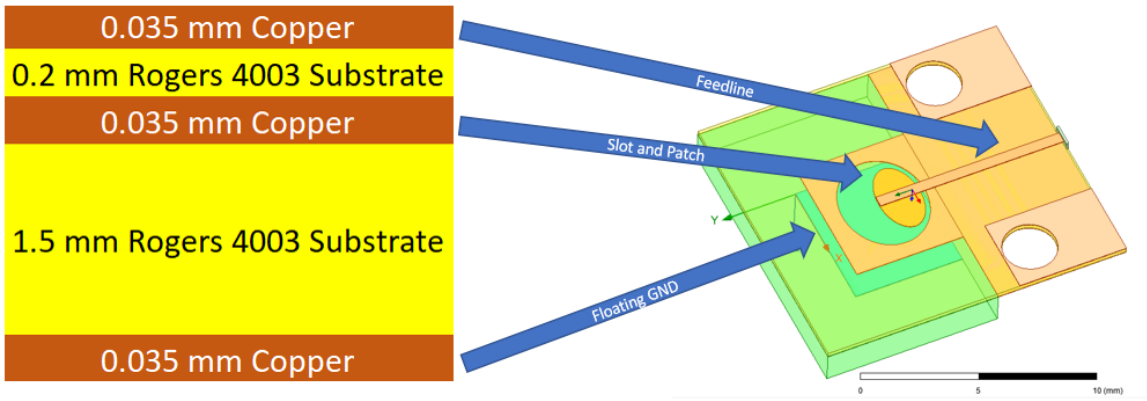

Figure 7: Finalized design with connector socket and elongated feed

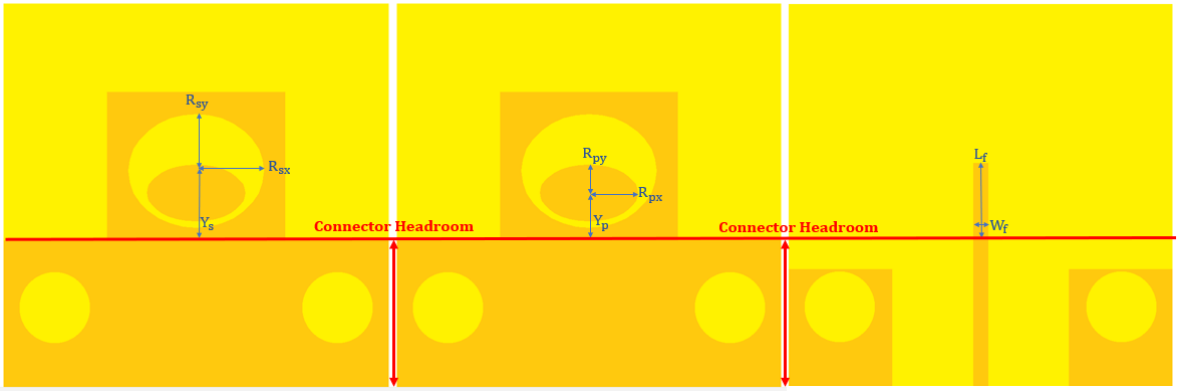

Figure 8: Critical length parameters for finalized design

Parameter	*Description*	*Value (mm)*
L_f	Length of the feedline	3.1
W_f	Width of the feedline	0.5
R_{px}	X radius of the patch	1.65
R_{py}	Y radius of the patch	0.96
Y_p	Y coordinate of center of the patch	2.1
R_{sx}	X radius of the slot	2.3
R_{sy}	Y radius of the slot	1.92
Y_s	Y coordinate of center of the slot	2.84

Table 1: List of crucial parameters for final design

After removal of the matching stub, addition of connector headroom, usage of different substrate and enlargement of substrate, the final design was able to have a bandwidth of 2.74 GHz centered at 27.89 GHz and results were shown in Figure 9. The realized gain was considered to include all the mismatch losses and achieved a 4.6 dBi gain over the bandwidth. The highest realized gain was observed at 28.5 GHz with 5.9 dBi and displayed in Figure 10. Realized gain was measured for $\varphi = 0^o$ and $\theta = 180^o$ and radiation patterns for $\varphi = 0^o$, $\varphi = 45^o$, $\varphi = 90^o$ and $\varphi = 135^o$ can be found in Figure 11. Back lobe radiation consists of two small lobes which are only visible for $\varphi = 0^o$ and the highest gain point is towards $\theta = 150^o$.

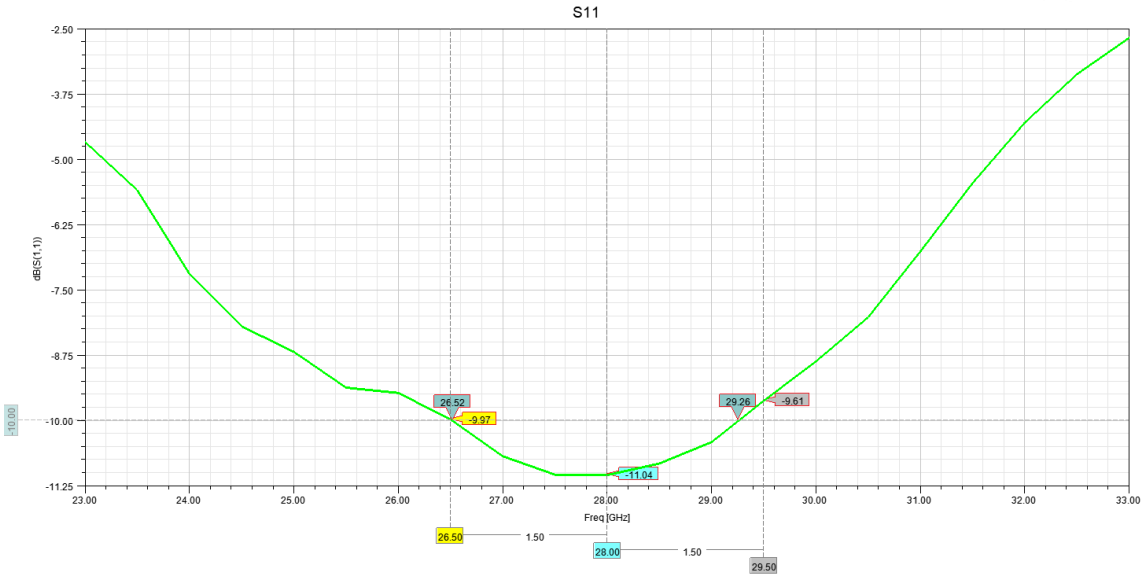

Figure 9: S11 of the final design

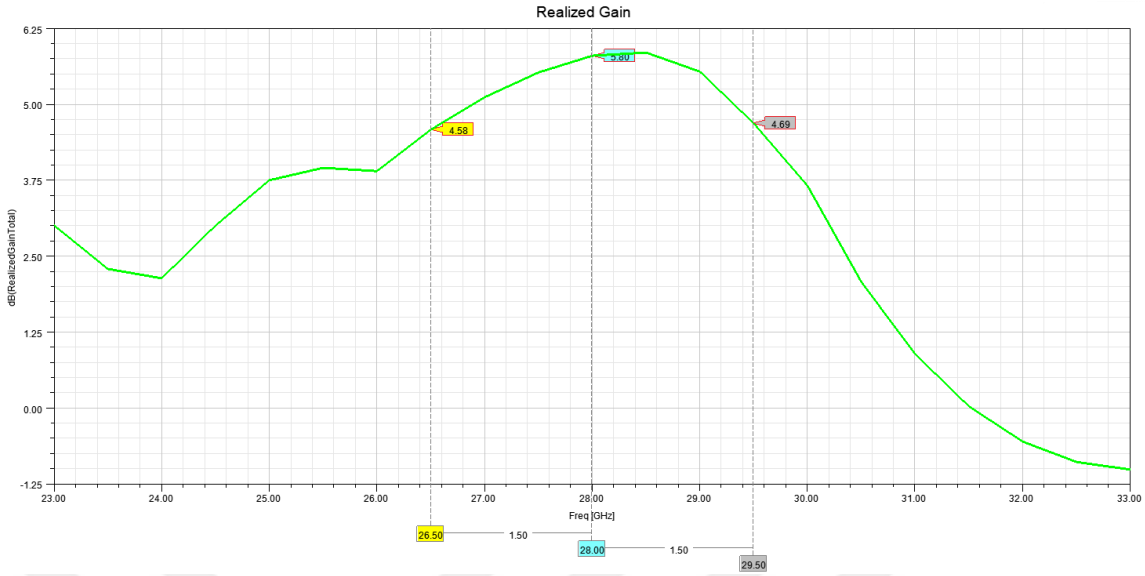

Figure 10: Realized gain for φ = 0° and θ = 180° of the final design over 23 – 33 GHz

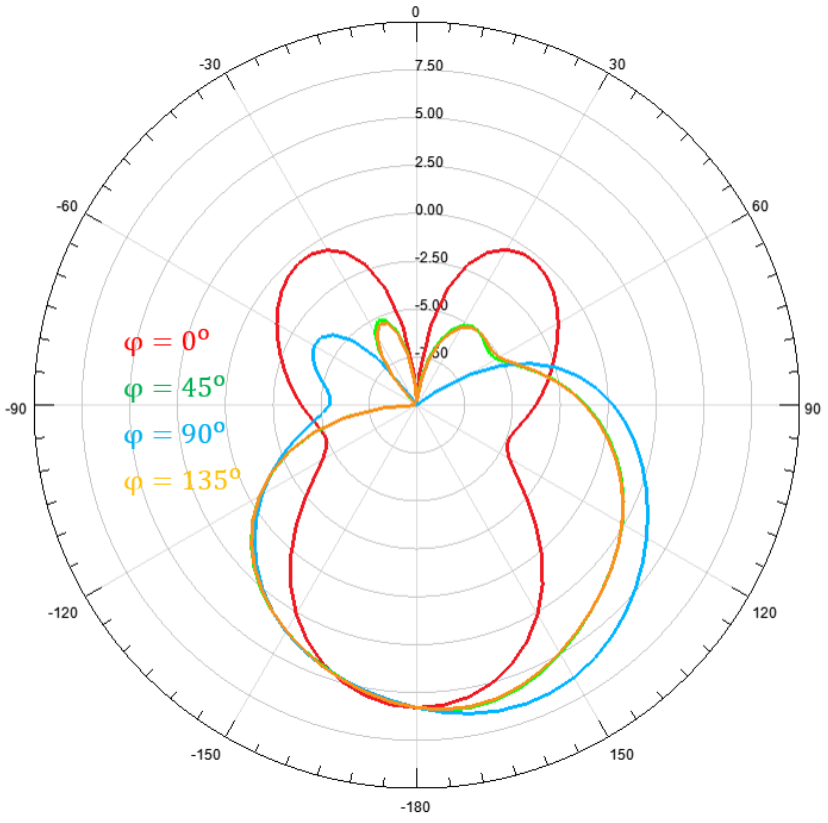

Figure 11: Final design's realized gain for φ = 0°, φ = 45°, φ = 90° and φ = 135° at 28 GHz

3.4. Results

The final antenna design was able to solve the problems observed in initial topology. Gain performance was improved to 4.6 – 5.9 dBi from 2 – 4 dBi while removing unwanted back lobe radiation. Additionally, removal of matching stub made the whole structure simpler to model, which is advantageous for machine learning tools in the next section. As expected, the broadband performance of the antenna was removed, but still showed enough bandwidth to cover commonly used n257 band. Some performance degradation was expected due to increased feedline length, but it was in the range of theoretical estimations [23].

Even though the improvements are remarkable, addition of another layer makes the whole structure 3 layered, which is not a standard practice in PCB manufacturing. The requirement of headroom for edge mount coaxial feeding also makes whole design a little bit awkward for system integration. Nevertheless, the antenna performance is in line with the anticipations and a detailed comparison with other works in the literature can be seen in Table 2. Works in Table 2 with single gain value indicates the maximum gain observed in the given bandwidth.

	Frequency (GHz)	*Bandwidth (GHz)*	*Gain (dBi)*	*Element Count (Array / Single)*
This Work	27.89	2.74	4.6 – 5.9	Single
[18].	28	2	12.5	8
[19]	28	1.5	10	4
[20]	27.5	2	9.5	4
[21]	30	20	2 - 4	Single
[24]	28	2	8 - 11	4
[25]	18	1	5	Single
[26]	21.5	1	5.3	Single
[27]	28.75	0.66	18.41	16

Table 2: Comparison with the other works in the literature

ANTENNA DESIGN WITH MACHINE LEARNING

This section of the thesis will cover the steps for designing an antenna with machine learning. The section will start with a discussion of the expected performance of the machine learning and design steps will be introduced shortly. Important aspects of the process such as dataset generation and algorithm evaluation will follow. Results of the proposed method will be presented, and a comparison will be done with respect to traditional methods.

4.1. Design Flow and Goals

The main argument of the thesis to achieve better performing antennae with a shorter time span. To build upon this idea, the goals of this section can be listed as:

- Antenna designed by the machine learning tool must have better performance in overall. By better, it strictly means a higher realized gain and lower reflection coefficient over the frequency band. The degree of improvement is not strictly defined because:
    - Initial design performs better than the other examples in the literature, so comparison with the state of art is not meaningful.
    - Antenna design is based on trade off principle like many other disciplines. An antenna cannot be improved without degrading other properties, so this work does not expect to have gain performance of an array configuration, which is unrealistic.

- The time aspect is a crucial part of the argument. It is established that machine learning tools only use a model to make a prediction, unlike simulation software which must calculate all the electromagnetic effects. Due to this operational difference, it is expected from machine learning tools to output results one order of magnitude faster than the traditional simulation tools.

- The mismatch losses are considered for the calculation of realized gain, so the proposed method must be able to generate multioutput results. Separate models for separate output parameters are not accepted.

To fulfill these goals, the first step will be dataset generation and a discussion about dataset properties will be presented. Hardware and software used will be detailed to establish a common ground. A brief description will be told about the available algorithms and their performance will be evaluated to decide among them. After the establishment of the algorithm, a score metric will be defined to quantify the success of the algorithm. The chapter will be concluded with results after the detailed explanation of the proposed method.

4.2. Dataset Generation and Properties

Table 1 includes key aspects of the proposed antenna which will be used as inputs of the machine learning algorithms. Another input will be the frequency of the simulation done. All the designs will be simulated from 23 GHz to 33 GHz with 0.5 GHz intervals and each frequency will correspond to a single entry to the dataset. For the outputs, two most important parameters, S11 (reflection coefficient) and realized gain (RG) will be recorded for each entry. Realized gain will be measured at position $\varphi = 0^o$ and $\theta = 180^o$ which is the direction orthogonal to the radiating surface. Dataset has 9 input parameters and 2 output parameters, which are shown in Table 3. Lengths are displayed in millimeters, frequency has an unit of GHz and output parameters shown with dB.

Input Parameters									Output Parameters	
L_f	W_f	R_{px}	R_{py}	Y_p	R_{sx}	R_{sy}	Y_s	Freq	S11	RG

Table 3: Parameters found in the dataset

Dataset contains 6081 datapoints and each datapoint corresponds to a S11 and a realized gain measured at a single frequency with given lengths. Each design will have S11 and realized gain results from 23 GHz to 33 GHz, which corresponds to 21 datapoints with 0.5 GHz intervals. From a design perspective, the dataset contains 289 unique designs. Each parameter's mean, standard deviation, minimum value, maximum value, and values at 25%, 50% and 75% are shown in Table 4.

	L_f	W_f	R_{px}	R_{py}	Y_p	R_{sx}	R_{sy}	Y_s	*Freq*	*S11*	*RG*
Mean	3.03	0.46	1.43	0.95	2.24	2.24	1.94	2.75	28.00	-6.86	2.59
StD	0.41	0.12	0.29	0.15	0.22	0.16	0.12	0.14	3.03	4.24	1.94
Min	1.50	0.1	0.3	0.40	1.85	1.60	1.60	2.44	23.00	-38.97	-9.64
25%	2.70	0.45	1.4	0.96	2.10	2.20	1.90	2.70	25.50	-9.00	1.32
50%	3.10	0.50	1.5	0.96	2.15	2.30	1.92	2.80	28.00	-6.08	2.76
75%	3.50	0.50	1.65	1.00	2.30	2.30	2.00	2.84	30.50	-3.68	3.96
Max	3.50	0.70	1.75	1.20	3.10	2.70	2.40	3.00	33.00	-0.62	6.09

Table 4: Statistic properties of each parameter in the dataset

The dataset is generated by sweeping length parameters one by one with different values. Unfortunately, it is not feasible to simulate every available variation. Thus, there is not a uniform distribution among the data points. For example, W_f is 0.50 mm for both 50% and 75% value and R_{py} is 0.96 mm for both 25% value and 50% value. Even though machine learning algorithms are designed for handling non-uniform distribution, extra attention must be paid during the accuracy calculation. Another important point is the hardware and software used during this dataset generation. All the simulations are done with dense meshing for each frequency in HFSS and interpolation methods are not used. HFSS 2021 version was used with maximum accuracy settings and simulations are done with the hardware detailed in Table 5. 6051 datapoints are generated in a time span of 41 hours which corresponds to 24.3 seconds for each datapoint. 24.3 seconds will be taken as the basis for comparison with machine learning tools.

Processor	11th Gen Intel(R) Core(TM) i7-11800H @ 2.30GHz 2.30 GHz
Installed RAM	16.0 GB
System type	64-bit operating system, x64-based processor

Table 5: Hardware used for generation of the dataset

4.3. Algorithm Choice and Performance Evaluation

After the generation of the dataset, the next phase is the determination of the possible algorithms. It is expected to develop a mathematical model, which can predict 2 different outputs with 9 different inputs. This problem can be formulized as:

$$(y_1, y_2) = F(x_1, x_2 \dots x_9) \quad 4.1$$

Model F denotes the well-known regression problem in which the interaction between independent variables is displayed in the form of a mathematical model [28]. Even though regression is a general problem which machine learning algorithms focus on, there are a few algorithms that can do multioutput regression [29]. Major algorithms which can perform multioutput regression can be listed as:

- Linear Regression
- K-Nearest Neighbor Regression
- Decision Tree Regressor
- Random Forest Regressor

Among these algorithms, linear regression is the simplest one because of the first-degree polynomial model. This model can be represented as:

$$y = a_0 + a_1 x_1 + a_2 x_2 + \cdots + a_n x_n \quad 4.2$$

Even though it is a simple model, this model can be used to formalize real-life problems such as the relationship between GDP and unemployment rate as shown in Okun's law [30]. Unlike linear regression, K-Nearest Neighbour (KNN) checks the nearest K neighbors around the point of interest to guess the value of the prediction. A very basic visualization of this method is shown in Figure 12b, in which the value of the prediction

varies as K values change. A high value of K may result in underfitting by missing the patterns, while low values of K cause overfitting by including inaccurate data points [31] . The best choice of K depends on the test and must be found by trying multiple values.

Unlike KNN, decision trees divide the dataset space into sections to find the value of a prediction. The division of the space is done by various matrices in which the entropy is minimized [32]. The size of the tree and segmentation depend on the dataset and must be found by trial and error. The random forest can be seen as an improved version of decision trees, because it uses multiple smaller trees to find the best model. A basic illustration of decision trees and random forest algorithms is also given in Figure 12c and Figure 12d.

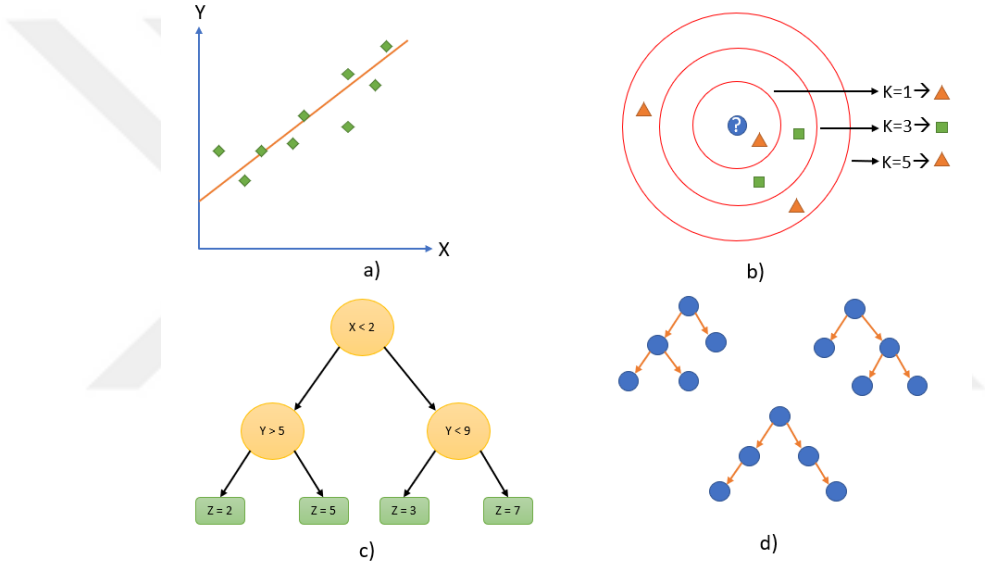

Figure 12: Illustration of multioutput regression algorithms: (a) Linear Regression, (b) KNN Regression, (c) Decision Tree Regressor and (d) Random Forest Regressor

To evaluate the performance of each algorithm, a 5-fold cross validation technique is used with a mean absolute value (MAE) as the success metric. Due to the simplicity of linear regression, it was chosen as a base model with a MAE of 1.98. For the KNN algorithm, algorithm type, leaf size and neighbor size hyperparameters are tuned as shown in Table 6 [33]. The best setup showed that on average there is a 0.67 dB difference between the real and predicted values of S11 and RG.

K = 2			K = 5			K = 10		
Type	*Leaf Size*	*MAE*	*Type*	*Leaf Size*	*MAE*	*Type*	*Leaf Size*	*MAE*
Ball	1	0.69	Ball	1	0.75	Ball	1	0.83
Ball	10	***0.67***	Ball	10	0.76	Ball	10	0.83
Ball	100	0.68	Ball	100	0.76	Ball	100	0.84
KD	1	0.68	KD	1	0.76	KD	1	0.84
KD	10	0.67	KD	10	0.76	KD	10	0.84
KD	100	0.70	KD	100	0.75	KD	100	0.84
Brute	1	0.71	Brute	1	0.75	Brute	1	0.82
Brute	10	0.69	Brute	10	0.76	Brute	10	0.84
Brute	100	0.73	Brute	100	0.76	Brute	100	0.84

Table 6: Hyperparameter tuning table for KNN algorithm

For decision trees, the same cross validation method was applied. The tuned parameters can be listed as the criterion, splitter choice, and samples required for splitting. After the hyperparameter tuning, the best MAE was observed as 0.52 dB. A summary of the hyperparameter tuning is shown in Table 7 [34].

Samples =2			**Samples = 5**			**Samples = 10**		
Criteria	*Splitter*	*MAE*	*Criteria*	*Splitter*	*MAE*	*Criteria*	*Splitter*	*MAE*
Square	Best	0.54	Square	Best	0.56	Square	Best	0.52
Square	Random	0.54	Square	Random	0.57	Square	Random	0.60
Friedman	Best	0.54	Friedman	Best	***0.52***	Friedman	Best	0.54
Friedman	Random	0.54	Friedman	Random	0.57	Friedman	Random	0.59
Absolute	Best	0.73	Absolute	Best	0.87	Absolute	Best	0.92
Absolute	Random	0.69	Absolute	Random	0.70	Absolute	Random	1.05
Poisson	Best	0.67	Poisson	Best	0.66	Poisson	Best	0.67
Poisson	Random	0.61	Poisson	Random	0.62	Poisson	Random	0.62

Table 7: Hyperparameter tuning table for decision tree algorithm

The random forest algorithm is also tuned with cross-validation as shown in Table 8. Criterion, estimator number, and samples required for splitting are tested with various values and setup with a squared error criterion, 100 estimators and 2 splitting samples showed the best performance with 0.5 dB error [35]. This setup also has the best performance among the algorithms which were used for the rest of the thesis.

Samples =2			Samples = 5			Samples = 10		
Criteria	*Estimator*	*MAE*	*Criteria*	*Estimator*	*MAE*	*Criteria*	*Estimator*	*MAE*
Square	50	0.51	Square	50	0.52	Square	50	0.53
Square	100	***0.50***	Square	100	0.52	Square	100	0.55
Square	200	0.51	Square	200	0.51	Square	200	0.55
Absolute	50	0.87	Absolute	50	0.89	Absolute	50	0.90
Absolute	100	0.86	Absolute	100	0.86	Absolute	100	0.92
Absolute	200	0.84	Absolute	200	0.88	Absolute	200	0.92
Poisson	50	0.56	Poisson	50	0.59	Poisson	50	0.62
Poisson	100	0.57	Poisson	100	0.59	Poisson	100	0.62
Poisson	200	0.57	Poisson	200	0.60	Poisson	200	0.62

Table 8: Hyperparameter tuning table for random forest algorithm

4.4. Score Metric

Machine learning tools can make many predictions in a short period. To compare each result, a systematic scoring method must be developed. First, a set of frequencies was created to evaluate the antenna designed at 28 GHz with 3 GHz bandwidth:

$$F = \{26.5\ , 27.0, 27.5\ , 28.0\ , 28.5\ , 29.0\ , 29.5\} \quad 4.3$$

S11 and RG values at the frequencies given in F were predicted with machine learning:

$$S_{11}(f)\ , f\ \epsilon\ F \quad 4.4$$

$$RG(f)\ , f\ \epsilon\ F \quad 4.5$$

The natural logarithm of the absolute value of S11 was taken and summed with the RG value at the given frequency as shown in Eq. 4.6. The S11 value below -10 dB was

accepted as well-matched impedance, so any value lower than -10 would overshadow the contribution made by RG. To negate this effect, natural logarithm was used.

$$Score(f) = \ln(|S_{11}(f)|) + RG(f)\ , f\ \epsilon\ F \tag{4.6}$$

Each score is summed up to find the final score of the design as shown in Eq. 4.7. This score metric gives a score of 53.92 for the antenna designed with HFSS. For machine learning tools, the goal is set to surpass 53.92.

$$\sum_{f} Score(f)\ , f\ \epsilon\ F \tag{4.7}$$

4.5. Iteration and Exhaustive Sweep

To start the proposed iterative process, a starting point must be chosen. This point can be a point in the dataset or an arbitrary point if the chosen length does not cause any physical overlap or intersection. This point can be defined as P_0, which has coordinates L_f, W_f, R_{px}, R_{py}, R_{sx}, R_{sy}, Y_p and Y_s as A_0, B_0, C_0, D_0, E_0, F_0, G_0 and H_0.

$$P_0(A_0, B_0, C_0, D_0, E_0, F_0, G_0, H_0) \tag{4.8}$$

To find the optimum lengths of the input parameters, they are grouped as pairs as the first step. Parameters which define the same object or property are put into the same group. For example, feed length and feed width both correspond to features of feedline. Thus, they are grouped as a Group 1. The grouping process can be seen in Figure 13.

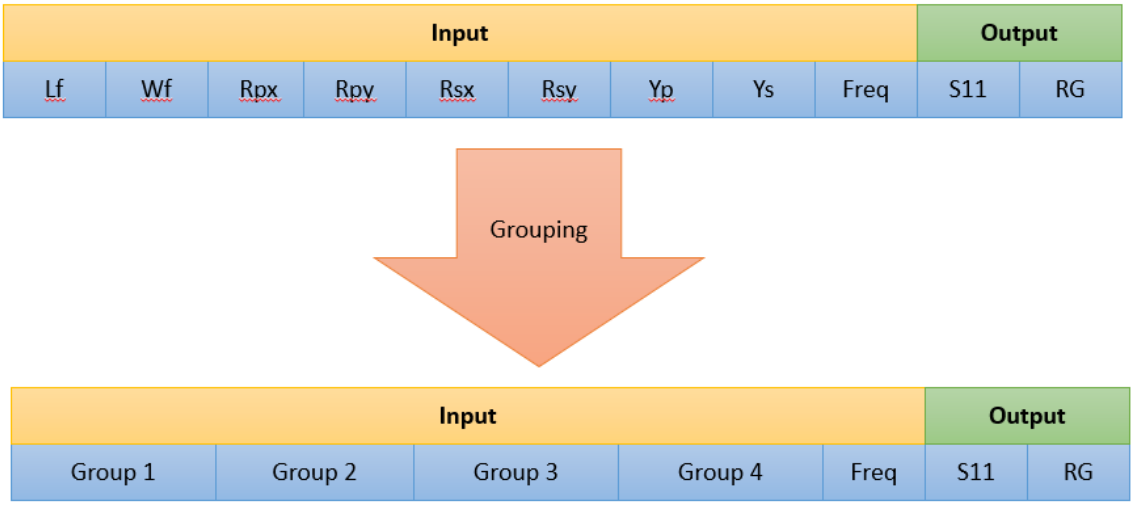

Figure 13: Grouping of input parameters

In Figure 14, S11 and RG were replaced with Group 1 and Group 1's place was taken by S11 and RG. With this setup, a machine learning model was trained.

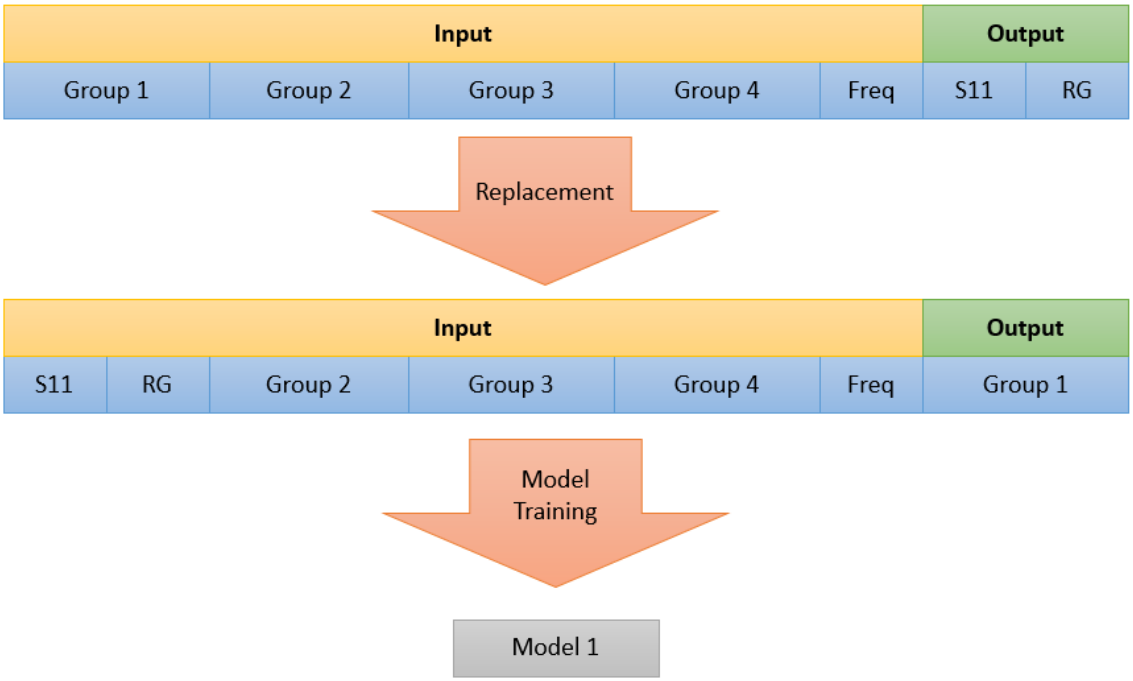

Figure 14: Parameter interchange and model training for Group 1

Parameters corresponding to Group 1 were removed from the initial design and they were replaced with S11 = -10 dB and RG = 5 dB. The reasoning behind these values is the

requirement of -10 dB S11 as impedance matching and 5 dBi realized gain being close to other works in the literature. Instead of predicting the performance values, length values are predicted, which is the core of the design process. The initial design is updated with the predicted values and design P_1 was generated. A summary of this step is shown in Figure 15.

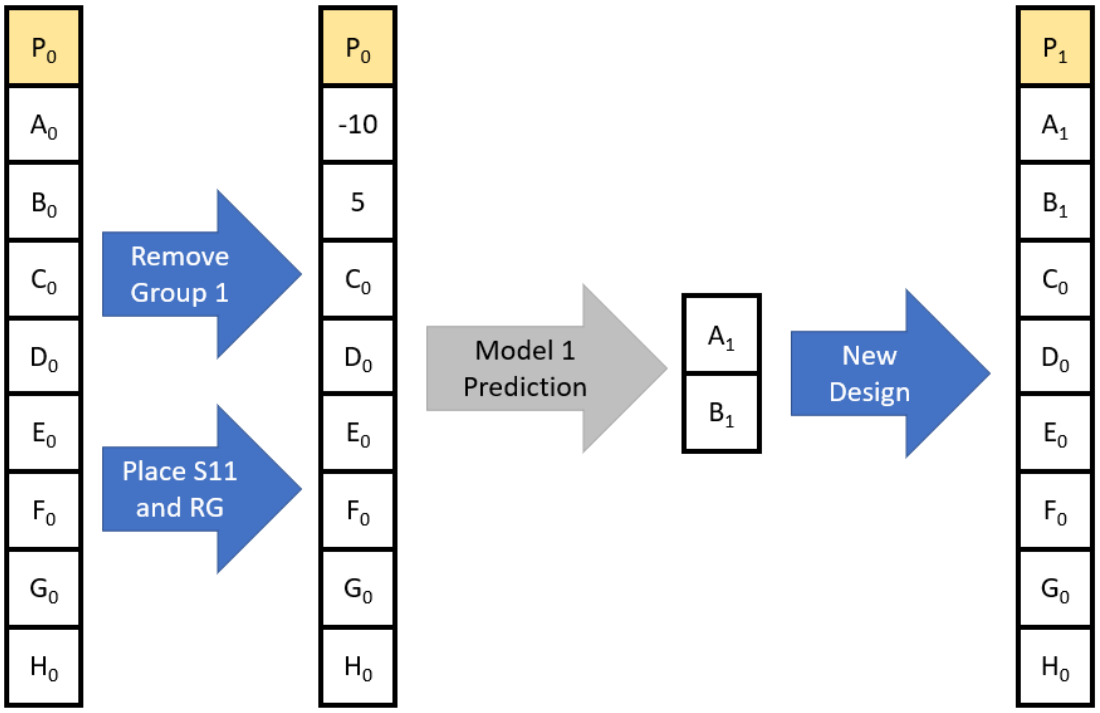

Figure 15: Generation of the second design with machine learning

The same procedure continued with the replacement of Group 2 with performance parameters. Another model was trained, and this model was used with design P_1 to predict C_1 and D_1. Prediction of C_1 and D_1 concluded with design P_2. Generation of the second model is shown in Figure 16 and design P_2 can be seen in Figure 17.

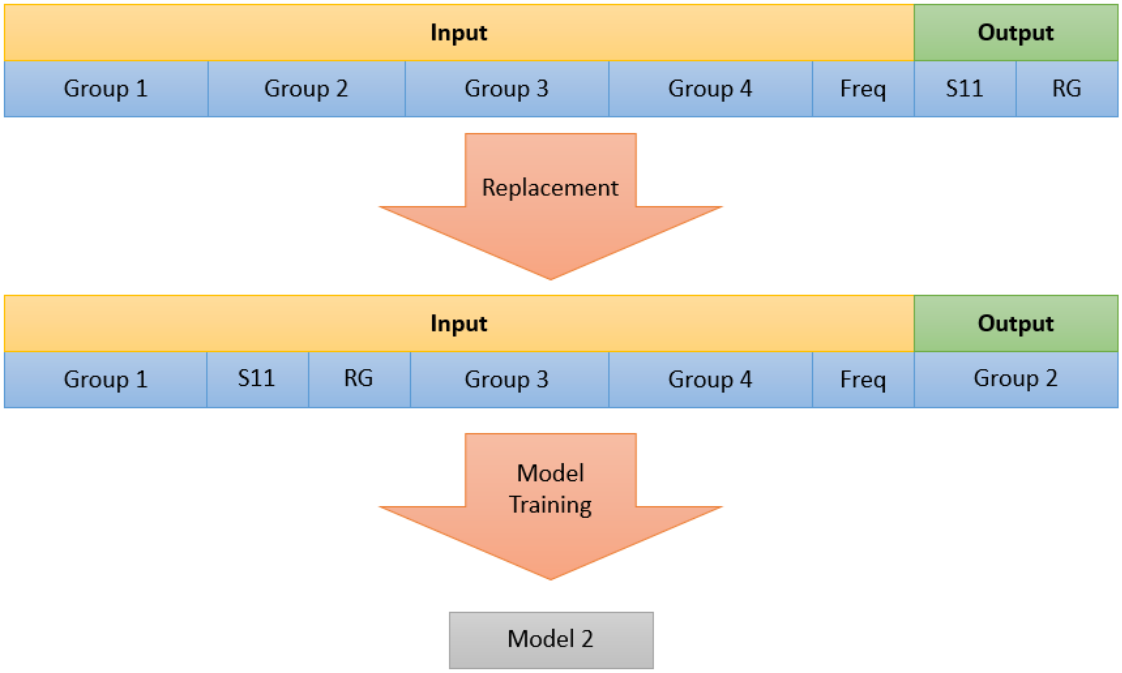

Figure 16: Generation of the second model with machine learning

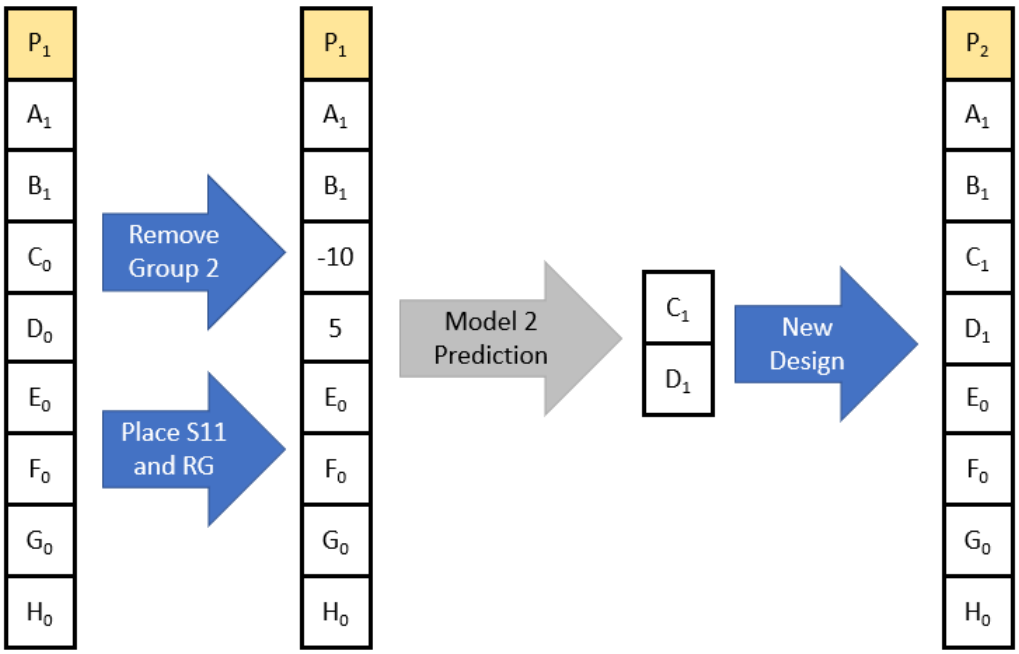

Figure 17: Generation of the third design

The proposed iterative method can be continued indefinitely, but a convergence criterion must be chosen. To complete the iteration:

- The last five models' scores must be within 2 points compared to each other. These scores are calculated with respect to the score metric defined in the previous section.
- The final score must be higher than 53.92 which is the score of the design done with HFSS.

It is important to note that the design found in the end of the iteration is not the end of the process. Parameters of the result of the iteration will be swept to +3% and -3% their values to check for any better design. The choice of 3% is done to prevent any intersection issues and the result of the exhaustive research will be the final design.

4.6. Results

After the iteration process, a design with a score of 55.34 was achieved in the 8th version. The score was over 53.92 and remained within 2 points in the last five iterations. The results table can be found in Table 9 and each update is shown in bold. To show the effect of each update, the contribution of S11 and RG is displayed separately in Figure 18.

Design	*Lf*	*Wf*	*Rpx*	*Rpy*	*Yp*	*Ys*	*Rsx*	*Rsy*	*Score*
P_0	2.5	0.45	1.50	0.90	2.30	2.6	2.00	2.00	29.10
P_1	**2.96**	**0.43**	1.50	0.90	2.30	2.6	2.00	2.00	28.32
P_2	2.96	0.43	**1.58**	**0.91**	2.30	2.6	2.00	2.00	30.09
P_3	2.96	0.43	1.58	0.91	**2.10**	**2.84**	2.00	2.00	49.32
P_4	2.96	0.43	1.58	0.91	2.10	2.84	**2.29**	**2.00**	53.69
P_5	**3.14**	**0.46**	1.58	0.91	2.10	2.84	2.29	2.00	53.66
P_6	3.14	0.46	**1.69**	**0.96**	2.10	2.84	2.29	2.00	54.19
P_7	3.14	0.46	1.69	0.96	**2.10**	**2.83**	2.29	2.00	55.50
P_8	3.14	0.46	1.69	0.96	2.10	2.83	**2.30**	**2.07**	55.34

Table 9: Iteration results of machine learning

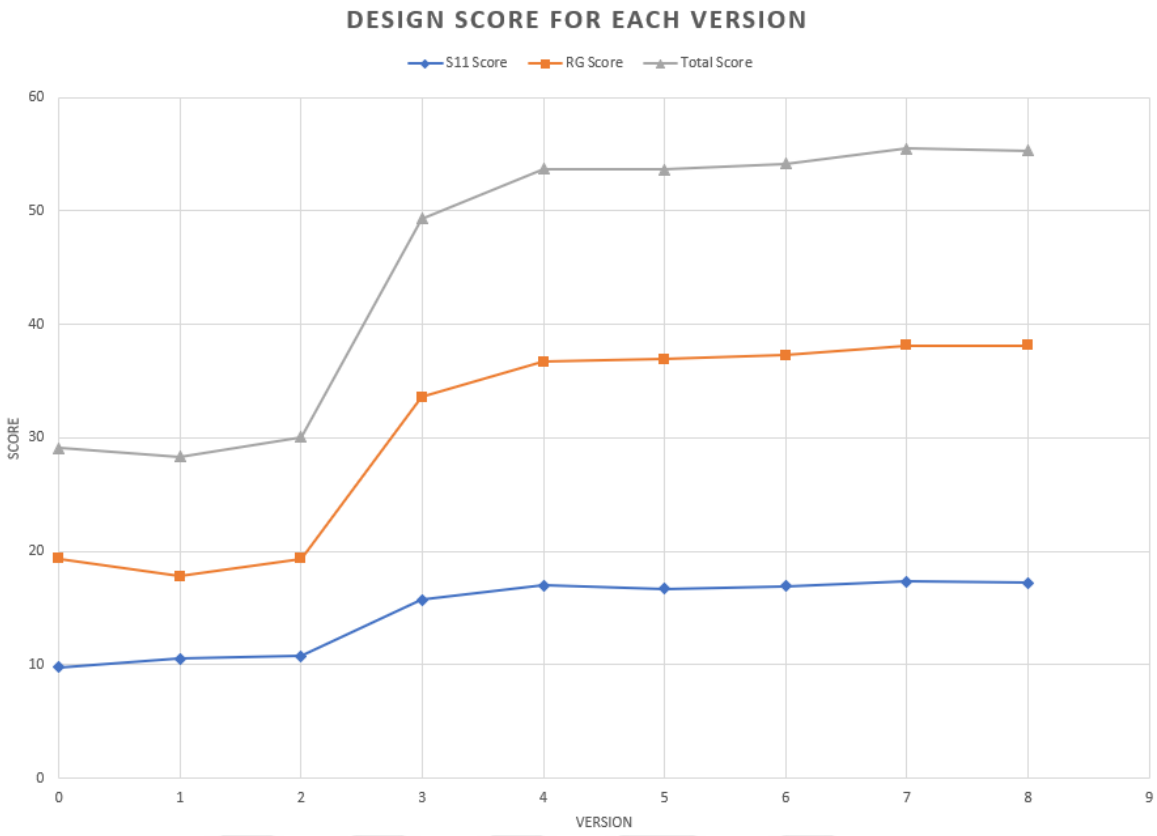

Figure 18: S11, RG and total score of each design version

Design P_8 was chosen for exhaustive sweep and each parameter was tested for three different values. A total of 6561 designs were tested in 22.6 minutes and the best result with a 56.03 score, is shown in Table 10.

Design	*Lf*	*Wf*	*Rpx*	*Rpy*	*Yp*	*Ys*	*Rsx*	*Rsy*	*Score*
P_{final}	3.14	0.44	1.77	0.96	2.1	2.84	2.40	2.00	56.03

Table 10: Best result of exhaustive sweep

The iteration process took 37 minutes to complete, so the prediction of 6570 points and finding a result of 56.03 required 59.6 minutes. Each design has 21 different frequency values, so 137970 different performance predictions were made for various designs at various frequencies. This corresponds to 0.026 seconds for each calculation. A comparison with the design of HFSS can be seen in Table 11. Both calculation time and score results indicate that the algorithm can achieve the desired results.

	Calculation Time (s)	*Score*
HFSS	24.3	53.92
Machine Learning	0.026	56.04

Table 11: Comparison of machine learning with traditional design method

DEEP LEARNING AND NEURAL NETWORKS

Desired results were achieved with machine learning algorithms, but the improvement seen in the results corresponds to only a 1 – 2 dB increase. To achieve a higher score, a neural network will be used. Neural networks are inspired from neuron structures, and they are capable of modelling complex problems with various layers and neuron configurations. This chapter will cover the development of a neural network and results achieved from both the neural network and deep learning will be compared.

5.1. Neural Networks

Neural networks were proposed as learning tools based on the structure of a neuron. Neuron is made of consecutive sections and the incoming signal is sent to the next section if it fulfills the activation requirement. Similarly, a neural network takes the input parameters as an incoming message. Then each parameter is sent to a neuron with different weights. These neurons are in hidden layers between input and output. A neural network with 1 input layer, 2 hidden layers and an output layer is shown in Figure 19 as an example. It is important to note that each output of a layer is sent to the next layer with weights. Inclusion of the weights can be seen as coefficients used in a linear regression problem [36]. For example, inputs of the first hidden layer in Figure 19 can be represented as:

$$a_1x_1 + a_2x_2 + a_3x_3 \; for \; F_1(X) \tag{5.1}$$

$$b_1x_1 + b_2x_2 + b_3x_3 \; for \; F_2(X) \tag{5.2}$$

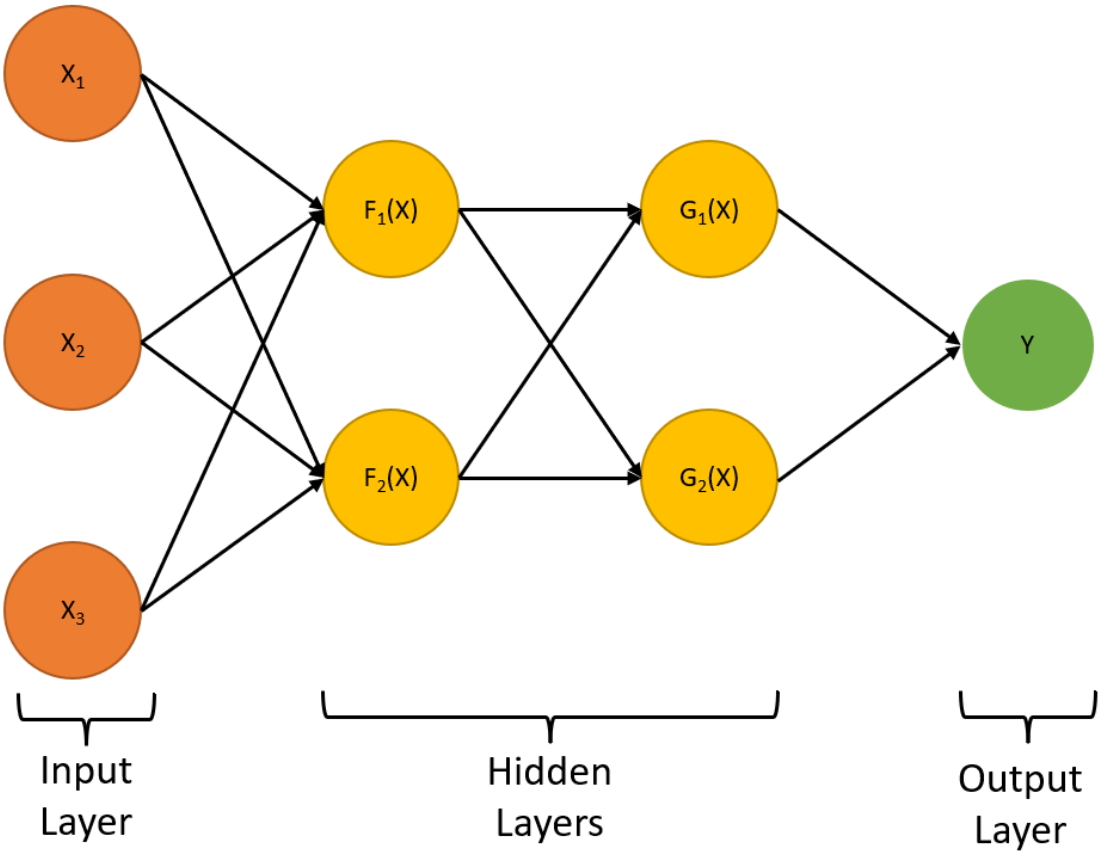

Figure 19: An example of a neural network with four layers

Each neuron takes the weighted input parameters and passes through a function like a neuron cell. If the weighted input can activate the function and an output is created. Then the output is also weighted and sent to the next neuron and the cycle continues. Even though the core mechanism of each neuron is based on linear regression, by changing the number of neurons in each layer and layer count, complex models can be achieved. For example, the output of $G_1(X)$ shown in Eq. 5.3 is not a simple linear model anymore.

$$G_1(c_1 * F_1(a_1x_1 + a_2x_2 + a_3x_3) + c_2 * F_2(b_1x_1 + b_2x_2 + b_3x_3)) \quad 5.3$$

The key difference between machine learning and deep learning is deep learning's capability of creating various complex models with the usage of neural networks. This capability can be used to create more complex models for the problem proposed in this thesis. Like machine learning, the best structure for a neural network depends on the dataset and the problem itself, so a trial-and-error method is required to find the best structure. Before that, some rule of thumb concepts must be considered:

- Without any hidden layer, a neural network is a linear regression algorithm which can be used for linearly dependent systems. Inclusion of a single layer can be used to model higher degree relations. Two or more layers are used for systems that are complex and have many dependent relations. It is important to note that each layer increases the complexity of the learning process. Thus, the system must be kept as simple as possible.

- For neurons in each layer, the choice depends on the dataset and the problem itself. To keep the complexity as low as possible, a neuron number that is less than the input number and greater than the output number is good practice.

Considering these rules of thumbs, a neural network with 1 input layer, 2 hidden layers and an output layer was created. The input layer contained 9 input parameters used in the machine learning part and the output layer had 2 parameters, which were RG and S11. For hidden layers, various neuron configurations are tested in Table 12, in which columns denote the number of neurons in first hidden layer and rows denote the number neurons in the second hidden layer. Each validation loss is calculated with 5-fold cross validation and the lowest loss (0.58) with 6 neurons in the first hidden layer and 6 neurons in the second hidden layer was chosen as the final topology.

L2 \ L1	3	4	5	6	7	8
3	0.76	0.63	0.67	0.74	0.66	0.70
4	0.64	0.72	0.63	0.75	0.67	0.73
5	0.82	0.70	0.71	0.63	0.72	0.80
6	0.78	0.60	0.62	**0.58**	0.71	0.67
7	0.67	0.64	0.67	0.63	0.65	0.74
8	0.63	0.65	0.73	0.68	0.77	0.65

Table 12: Validation loss of the proposed neural network with various neuron numbers for each hidden layer

5.2. Comparison with Machine Learning

Iteration with machine learning was able to give a score higher than a traditionally designed antenna, but it improved the results by only a few points. To improve performance, a hybrid approach was adopted. Machine learning for iteration and deep learning for exhaustive sweep was used. As a starting point for sweeping, the results found in Table 9 were used. The setup for exhaustive sweep was applied without a change and it took 312.6 minutes to test 137970 predictions. Due to more complex structure of neural networks, it was expected to have longer computation time and expectations were met with a nearly 14-fold increase in the exhaustive sweep time. The whole process took 345 minutes and the best result found was 57.72, which was higher than the result found with machine learning. A comparison of the results found with traditional design methods, machine learning and deep learning can be found in Table 18.

	Calculation Time (s)	*Score*
Machine Learning	0.026	56.04
Deep Learning	0.15	57.72

Table 13: Comparison of result found with traditional methods, machine learning and deep learning

NEW DESIGNS AT DIFFERENT FREQUENCIES

This chapter will cover the steps taken to design antennae at 25 GHz and 31 GHz instead of 28 GHz with learning tools. An initial statement of purpose will be declared to give a reasoning for steps taken and methods discussed in previous chapters will be applied. The chapter will be concluded with the results and comparison of learning methods.

6.1. Goals

Even though the results observed from deep learning and machine learning were superior compared to traditionally designed antennas, performance of the proposed method must be tried in other frequencies to fully see the improvement. Additionally, extra investigation must be done on initial iteration point to evaluate their effect on the proposed method. For these reasons:

- New designs will operate at 25 GHz and 31 GHz to show performance of the algorithms in full frequency spectrum.

- There is not an antenna traditionally designed for 25 GHz and 31 GHz, so design with the best score in the dataset corresponding to given center frequencies will be chosen as a point of comparison.

- Design with the highest score in the dataset will be used as the initial point for iteration. By starting from a point with a higher score, it is expected to improve the score in the iteration phase.

The original goals of achieving a higher score than the traditionally designed antenna, in this case it will be the antenna with the highest score in the dataset, and faster design time are also included as goals of this section.

6.2. Iteration and Exhaustive Sweep

As the initial step, the dataset was scanned for the best design for 25 GHz with a bandwidth of 3 GHz. The best design, which is shown as P_0 in Table 14, was used as the initial point. After 7 iterations, a score improvement from 48.49 to 48.83 was observed. The observed improvement was less remarkable than the improvement observed in the iteration phase of the 28 GHz design. Only W_f, Y_p and Y_s were updated, which explains the low change in the scores. The whole process was completed in 32 minutes and scores of each version can be seen in Table 14.

Design	*Lf*	*Wf*	*Rpx*	*Rpy*	*Yp*	*Ys*	*Rsx*	*Rsy*	*Score*
P_0	3.00	0.10	1.50	0.60	2.15	2.60	2.70	2.00	48.49
P_1	**3.00**	**0.097**	1.50	0.60	2.15	2.60	2.70	2.00	48.62
P_2	3.00	0.097	**1.50**	**0.60**	2.15	2.60	2.70	2.00	48.62
P_3	3.00	0.097	1.50	0.60	**2.04**	**2.45**	2.70	2.00	48.83
P_4	3.00	0.097	1.50	0.60	2.04	2.45	**2.70**	**2.00**	48.83
P_5	**3.00**	**0.097**	1.50	0.60	2.04	2.45	2.70	2.00	48.83
P_6	3.00	0.097	**1.50**	**0.60**	2.04	2.45	2.70	2.00	48.83
P_7	3.00	0.097	1.50	0.60	**2.04**	**2.45**	2.70	2.00	48.83

Table 14: Iteration steps of 25 GHz antenna with starting point as the best data point in the dataset

The same steps were repeated for the 31 GHz design and the best design in the dataset for 31 GHz was chosen as the starting point of the iteration. Like 25 GHz design, only L_f and W_f were updated one time and a score improvement of 46.36 to 46.54 was observed. The details about each iteration can be found in Table 15 and the whole iteration step was concluded in 23 minutes. A step-by-step score change of 25, 28 and 31 GHz designs were graphed in Figure 20 to display the effect of the initial point.

Design	*Lf*	*Wf*	*Rpx*	*Rpy*	*Yp*	*Ys*	*Rsx*	*Rsy*	*Score*
P_0	3.50	0.50	1.00	1.00	2.60	3.00	2.20	2.40	46.36
P_1	**3.40**	**0.46**	1.00	1.00	2.60	3.00	2.20	2.40	46.54
P_2	3.40	0.46	**1.00**	**1.00**	2.60	3.00	2.20	2.40	46.54
P_3	3.40	0.46	1.00	1.00	**2.60**	**3.00**	2.20	2.40	46.54
P_4	3.40	0.46	1.00	1.00	2.60	3.00	**2.20**	**2.40**	46.54
P_5	**3.40**	**0.46**	1.00	1.00	2.60	3.00	2.20	2.40	46.54

Table 15: Iteration steps 31 GHz antenna with starting point as the best data point in the dataset

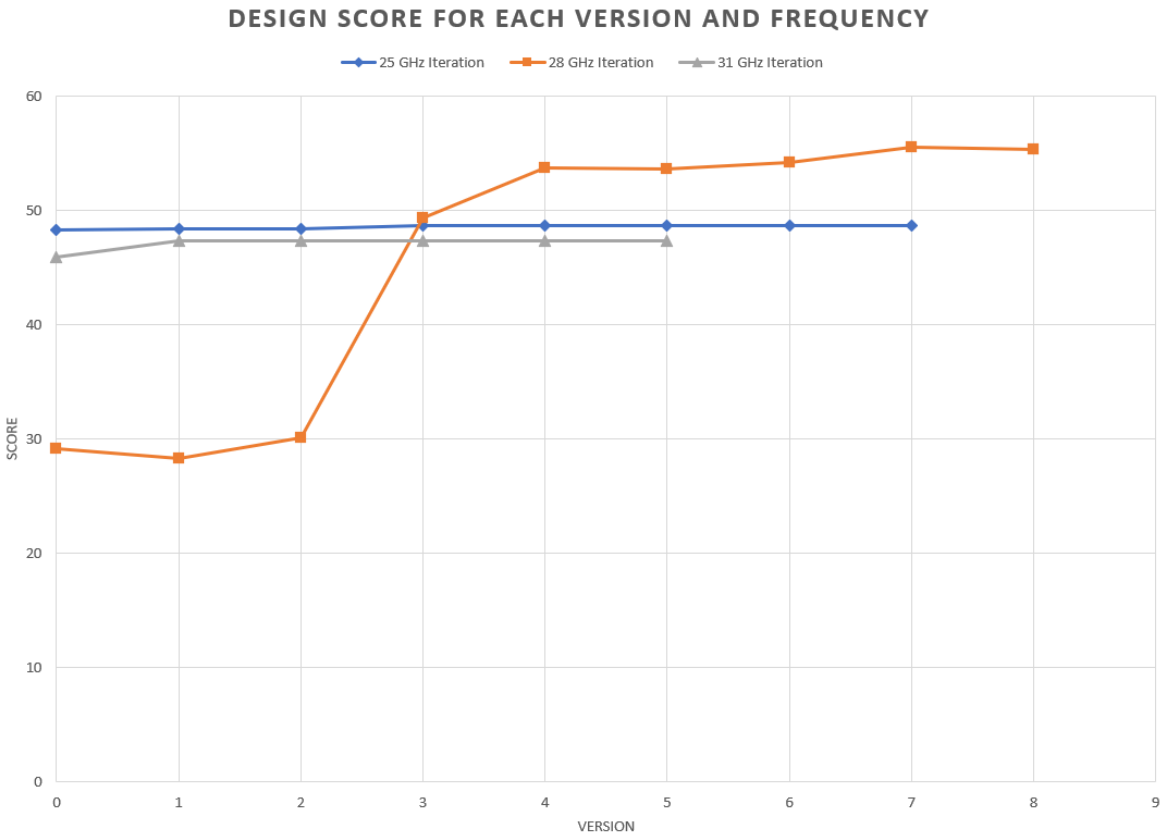

Figure 20: Design scores for iteration steps of 25, 28 and 31 GHz designs

Both designs were swept with machine learning and deep learning models as the next step. Each parameter was swept from 97% value to 103% with 3% steps, which made a total of 6561 different designs. Machine learning was able to complete the process in 24.3 minutes for 25 GHz design and 23.2 minutes for 31 GHz. On the other hand, the sweep process took 307 minutes for 25 GHz design and 299 minutes for 31 GHz design with deep learning. The results of each sweep is shown in Table 16.

Design	*Lf*	*Wf*	*Rpx*	*Rpy*	*Yp*	*Ys*	*Rsx*	*Rsy*	*Score*
ML_{25GHz}	3.00	0.103	1.50	0.60	2.09	2.52	2.70	2.00	50.13
DL_{25GHz}	3.09	0.10	1.55	0.62	2.02	2.60	2.78	1.94	51.21
ML_{31GHz}	3.40	0.48	1.00	1.00	2.60	3.00	2.20	2.40	48.35
DL_{31GHz}	3.5	0.47	1.03	1.03	2.52	3.00	2.27	2.47	47.23

Table 16: Machine and deep learning results of 25 GHz and 31 GHz designs

6.3. Results

After the completion of an exhaustive sweep, the total time spent was considered to calculate the time required for a performance parameter at a single frequency of a single design. Like the work done for 28 GHz, both machine learning and deep learning were faster than HFSS in the range of 10 – 100 folds. A score improvement from 48.88 to 50.13 and 51.21 were observed for the 25 GHz design. For 31 GHz, the score was increased to 48.35 and 47.23 from 46.84. Table 17 summarizes the results found in this chapter.

	Calculation Time (s)	*Score*
HFSS 25 GHz	24.30	48.88
HFSS 31 GHz	24.30	46.84
ML 25 GHz	0.025	50.13
DL 25 GHz	0.147	51.21
ML 31 GHz	0.020	48.35
DL 31 GHz	0.140	47.23

Table 17: Exhaustive sweep score values of 25 and 31 GHz designs with machine learning and deep learning

FABRICATION

This chapter will cover the fabrication steps done for antennae with the best performance at 25, 28 and 31 GHz. Preparations done before the fabrication will be told and problems encountered during the fabrication will be detailed. A brief description of the post fabrication process and measurement setup will be included. Measurement results will be given in a separate section in the following chapter to display every result in a single chapter.

7.1 Fabrication Preparations

For the fabrication process, RF connectors were placed to check if there is an intersection with the substrate. Placement of the connectors can be seen in Figure 21.

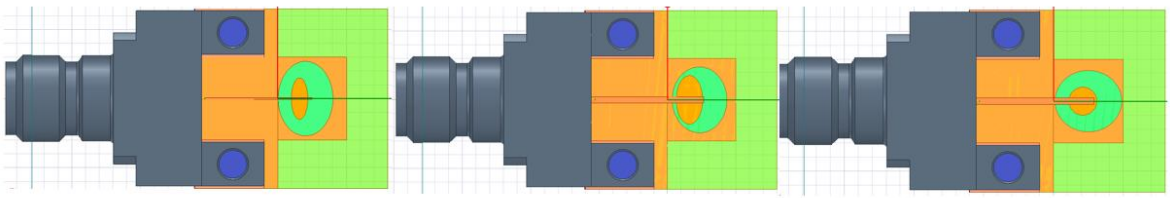

Figure 21: 25, 28 and 31 GHz designs with connectors

After the validation of the connector placement, all the designs were placed to a single PCB to facilitate the production phase. Additionally, the radiating and reflector part of the antenna was separated due to usage of different substrates. In Figure 22, the radiating layer with Rogers 4003 0.2 mm substrate is shown from bottom side. For connector holes, placeholder parts were shown with dull green parts. These parts were added to mark their location as drill points in Gerber files. The reflector layer of the antenna is also shown in

Figure 23. This layer consisted of small patches (shown in light blue) to reflect lobe radiation. Gerber files were taken for radiating and reflector layer and sent to fabrication.

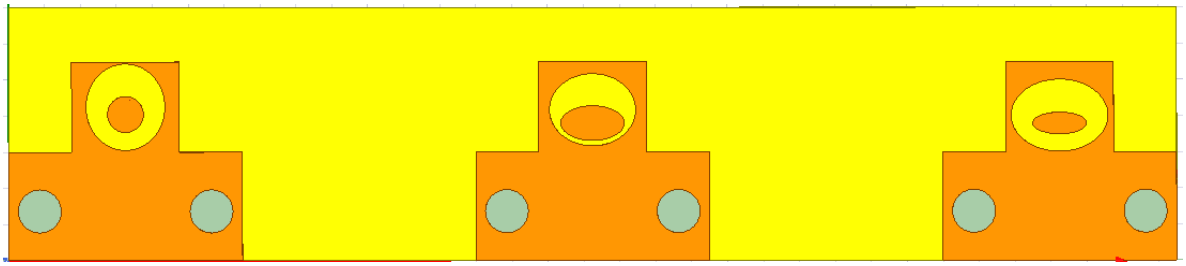

Figure 22: Radiating layer of the combined designs

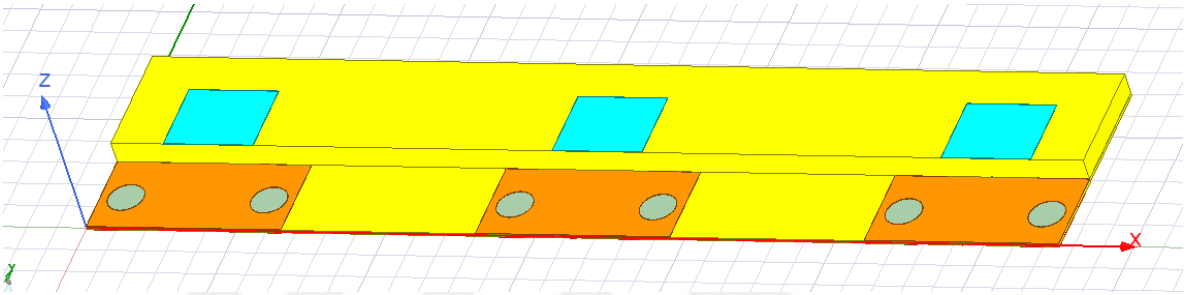

Figure 23: Reflector layer below the radiating part

7.2 Fabrication Phase

The fabrication process was done with a PCB milling machine, which was a common tool used for manufacturing PCB prototypes. Although these machines are capable of handling tolerances of 0.1 mm on less than 0.2 mm substrates, fabrication problems still occur. The first prototype for the radiating layer was shown in Figure 24. The main problems observed in the first prototype can be listed as:

- Torn patches. The metal density of the structure was very low compared to standard PCB fabrication. In most of the PCBs, large GND layers are kept in contact to keep the radiation from the transmission line constrained. For antennae, the opposite is aimed to have the highest degree of radiation. When the lack of metal density and thin substrate are combined, mechanical stability of the PCB is significantly decreased.

- Unfinished copper milling. The fact that large portions of copper must be milled, the tip of the milling tools can become blunt in a short time. To prevent this

situation, less sensitive but more durable milling tools were used for large copper areas. The disadvantage of this method is the accuracy of the milling depth. Too deep milling can penetrate the deep substrate and too thin milling can leave the copper in contact.

- Non-uniform transmission line thickness. Even though milling can be done with 0.1 mm accuracy, the feedline itself is 0.1 mm. Even a variation of 0.03 mm can result with 0.07 mm to 0.013 mm thick lines.

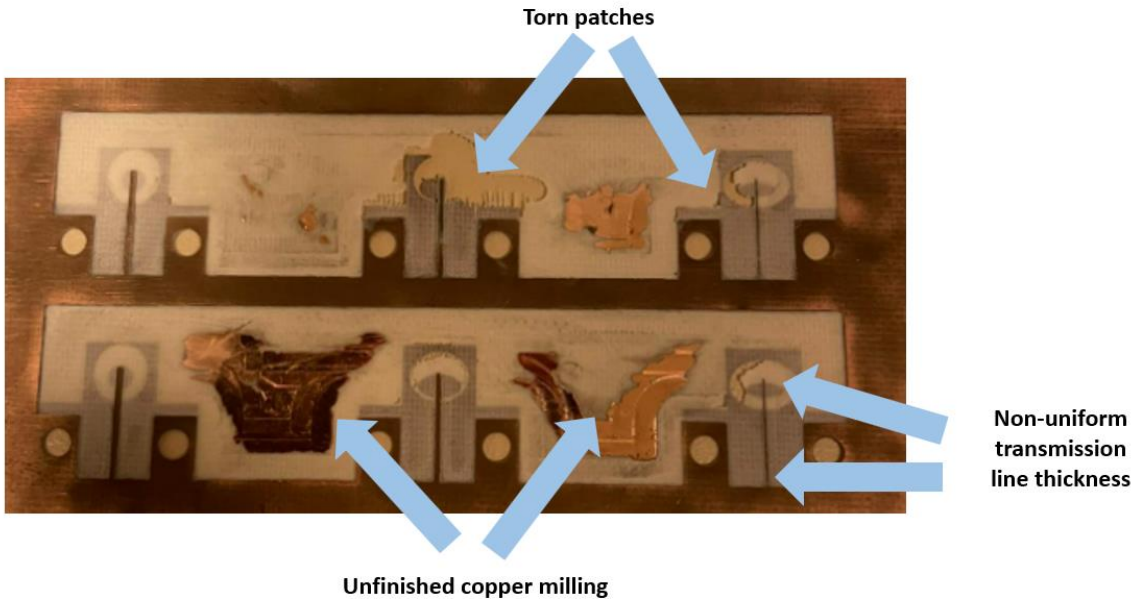

Figure 24: First prototype of the radiating layer with fabrication problems

After many fabrication trials, acceptable radiating layers were achieved in the 5th and 6th prototypes. For the reflector layer, there were not any problems with the fabrication.

7.3 Measurement Setup

After the fabrication of the antennae, it was decided that it would be better for measurements to separate each antenna from each other. As seen in Figure 25, parts separating reflectors and antennae were cut out. Additionally, some parts of the antennae were trimmed out to remove copper residues. Connector holes opened with needles and structures were combined with epoxy. Because of the effect of epoxy on the overall

substrate thickness, it was only applied to the sides of the antennae, not between layers. A clearer representation can be seen in Figure 25.

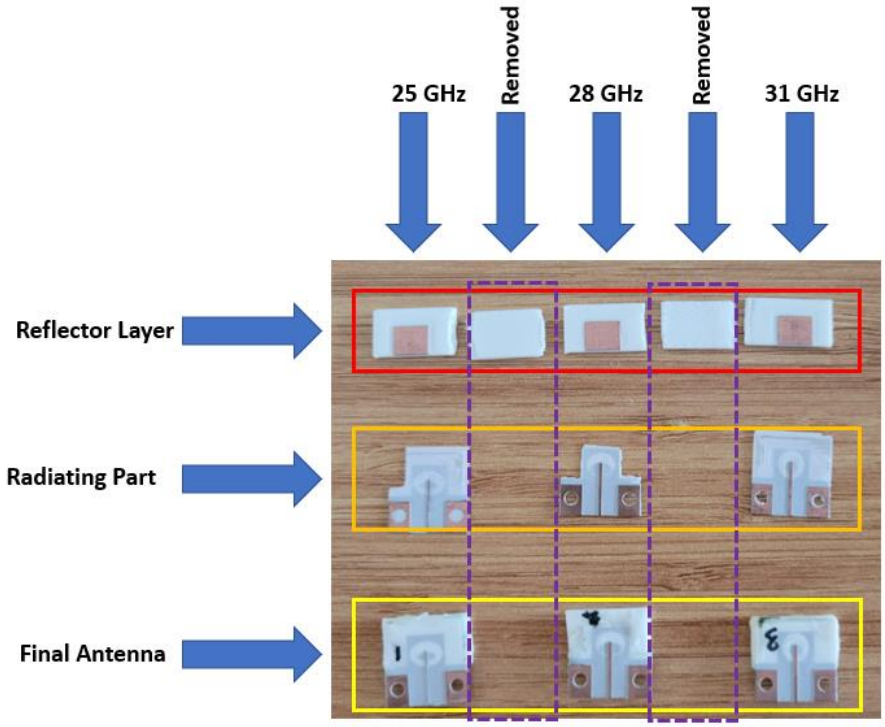

Figure 25: Final antennae for measurement with their reflector and radiating layers

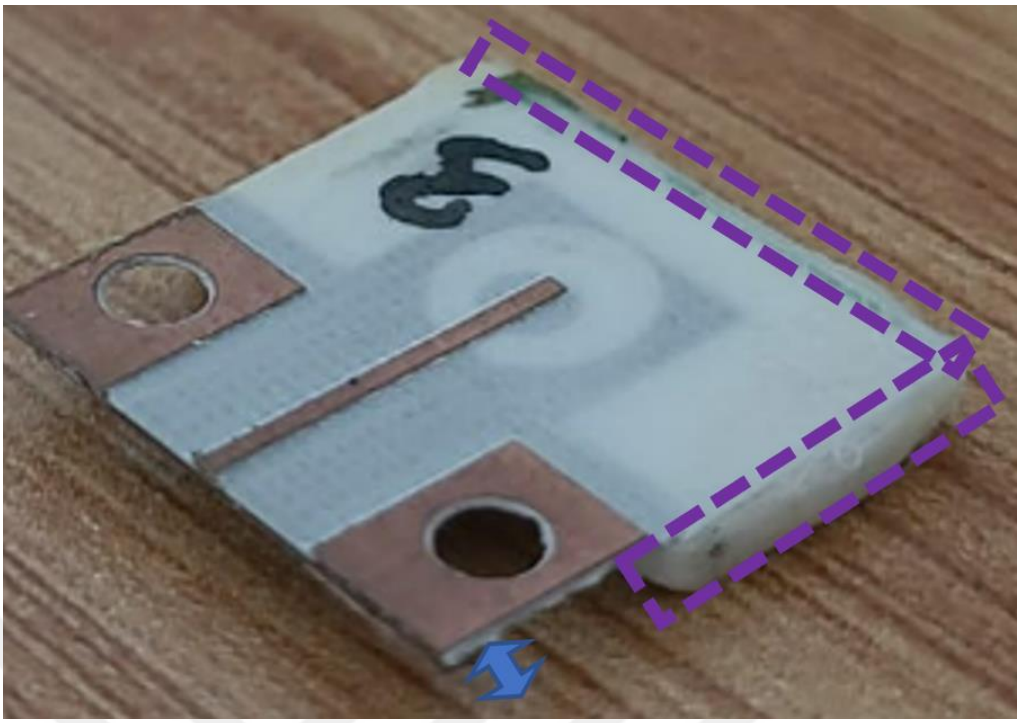

Figure 26: Close up view of 31 GHz antenna with epoxy residues (purple) and connector headroom (blue)

For the measurement, anechoic chamber located in SUNUM (Sabancı University Nanotechnology and Application Center) was used. This anechoic chamber uses a reference antenna to test the radiation pattern of DUT (Device Under Test). A reference antenna can be seen in Figure 27 and the DUT was located as shown in Figure 28. To measure radiation pattern and gain values, DUT was rotated in azimuth and elevation axis. This process was repeated for 28 GHz and 31 GHz and results can be in the Results Chapter.

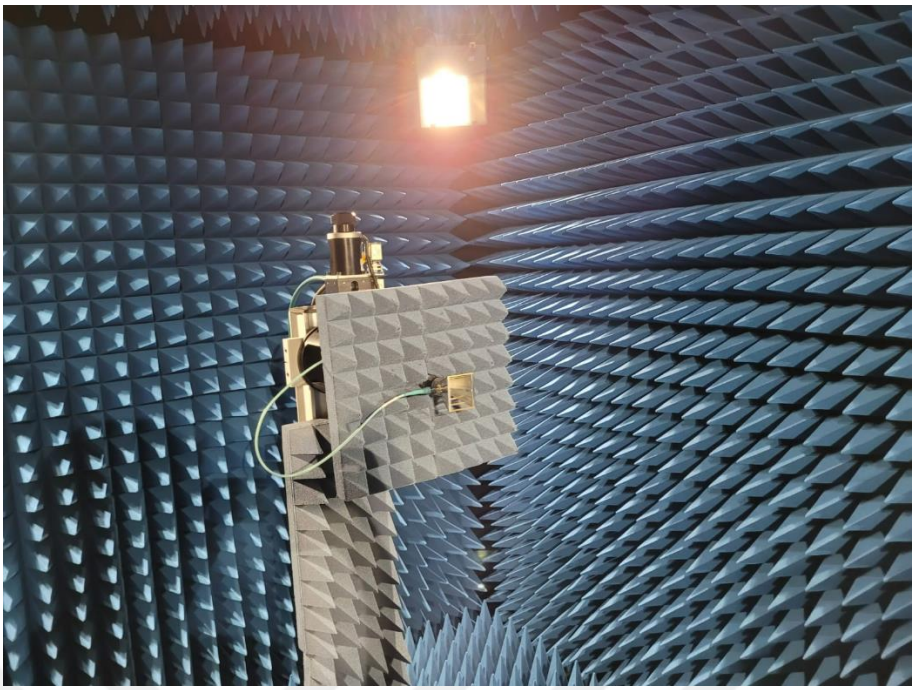

Figure 27: Reference antenna used in anechoic chamber

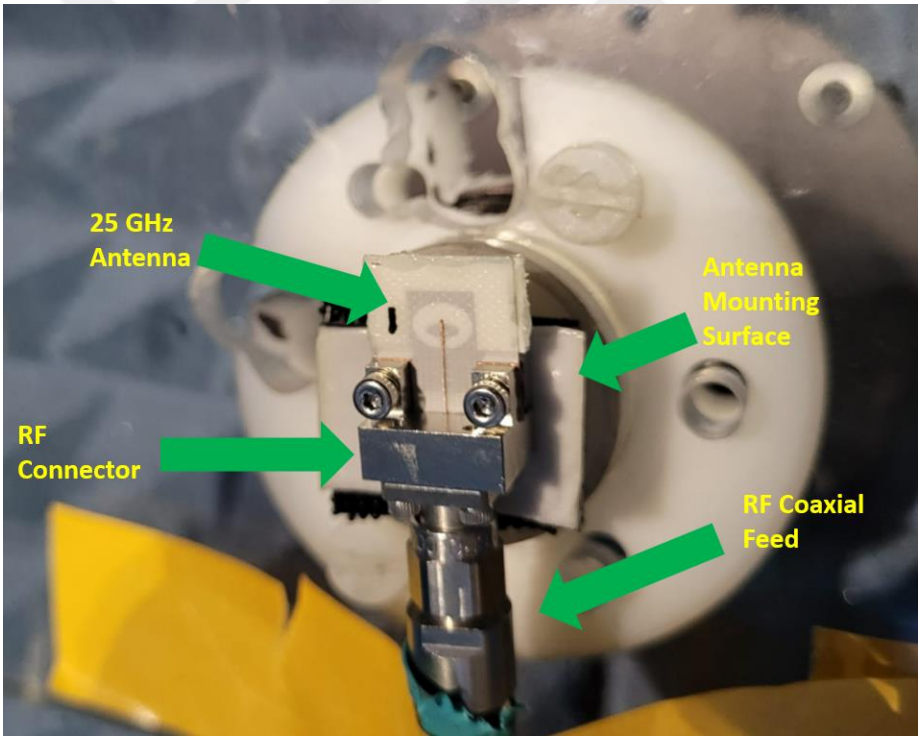

Figure 28: 25 GHz antenna in the measurement setup

RESULTS

Results of the designed antennae will be compared with the simulation results of HFSS to verify the accuracy of the proposed method. To follow order of design process, the 28 GHz design will be discussed first, and it will be followed by the 25 GHz and 31 GHz designs. After the comparison of the simulation results, fabrication results will be shown.

8.1. 28 GHz Design Results

Different designs with machine learning and deep learning were done and their performance were compared with the proposed score metric. As stated in section 4.3, a MAE of 0.50 dB was observed for the machine learning tools, which corresponds to a score variation of 3.5 in the worst-case scenario. To remove any uncertainties, proposed designs were tested with HFSS one more time and score values based on HFSS results were also shown. Additionally, the design with the highest score in the dataset was also displayed as another point of comparison. As seen in Figure 29, both machine learning and deep learning design have better matching compared to the traditional design and the best design found in the dataset. Although the deep learning design's center frequency was a little bit shifted to 29 GHz, it still had enough bandwidth for the 5G n257 band.

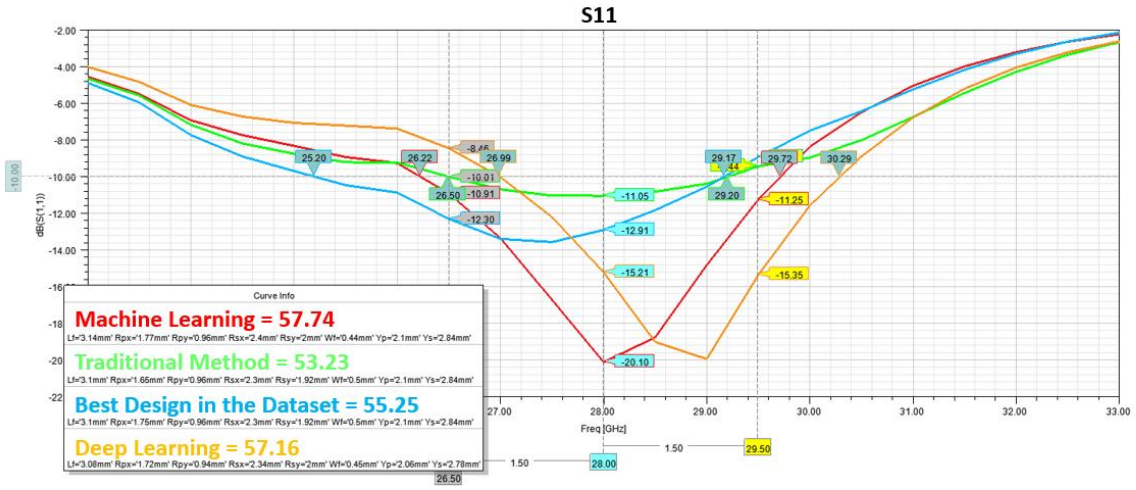

Figure 29: HFSS S11 results of machine learning design, traditional method design, best design in the dataset and deep learning design for 28 GHz

Realized gains of the proposed designs were shown in Figure 30. Every design had an average of 5 dBi gain in its bandwidth and the results are close to each other between 26.5 GHz to 28 GHz. The real difference was observed at 29.5 GHz, in which both machine learning and deep learning design have higher gains.

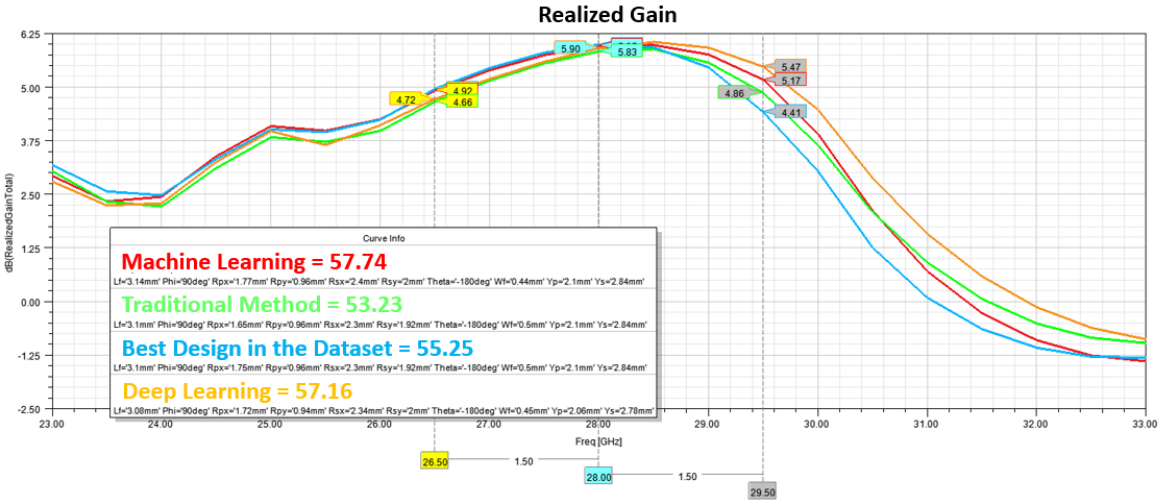

Figure 30: Realized gains of machine learning design, traditional method design, best design in the dataset and deep learning design for 28 GHz

8.2. 25 GHz and 31 GHz Design Results

Like the previous section, designs for 25 GHz were simulated with HFSS to see the exact performance. In Figure 31, S11 performance of learning algorithms were not as good as the best design in the dataset. The deep learning design's center frequency was shifted down to the lower end of the bandwidth and machine learning's S11 values are lower than the best design in the dataset. Even though S11 performance is not remarkable, machine learning and deep learning still have slightly higher scores. The reason behind this phenomenon can be seen in Figure 32. In every frequency of interest, both machine learning and deep learning design have 0.1 – 0.3 dB higher gains. Due to a low increase in realized gain values and slight performance degradation in S11, proposed designs have score values very close to the best design in the dataset.

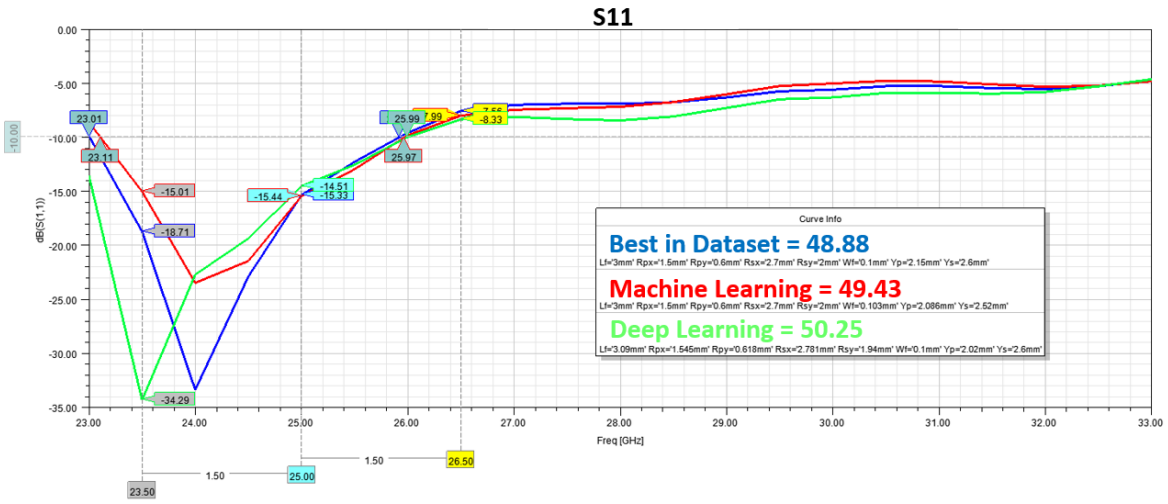

Figure 31: S11 of 25 GHz designs for machine learning, deep learning, and the best in dataset

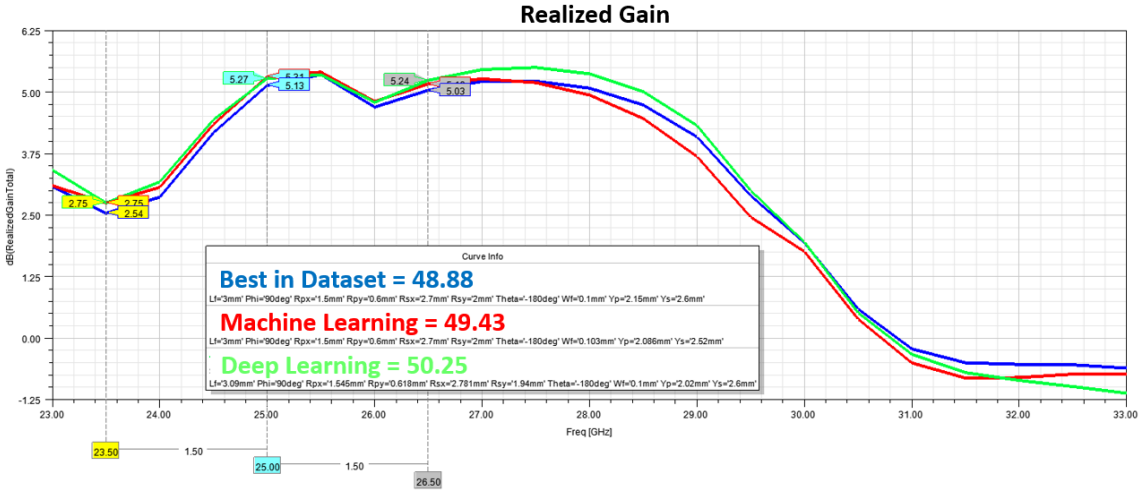

Figure 32: RG of 25 GHz designs for machine learning, deep learning, and the best in dataset

31 GHz machine learning and deep learning design were also simulated with HFSS and their S11 results can be seen in Figure 33. Unlike 25 GHz, machine learning improved S11 and the graph has a shape very similar to the best design in the dataset. Deep learning also had better S11 results, which were closer to 31 GHz center frequency compared to other designs. When realized gain values were checked, machine learning had 0.1 – 0.3 dB gain over the whole frequency band as shown in Figure 34. Deep learning design had a different behavior in which higher gain values were observed for the lower end of the bandwidth and lower gain values for the higher end of the bandwidth. Due to slight improvement in both S11 and RG, machine learning was able to give designs with higher scores.

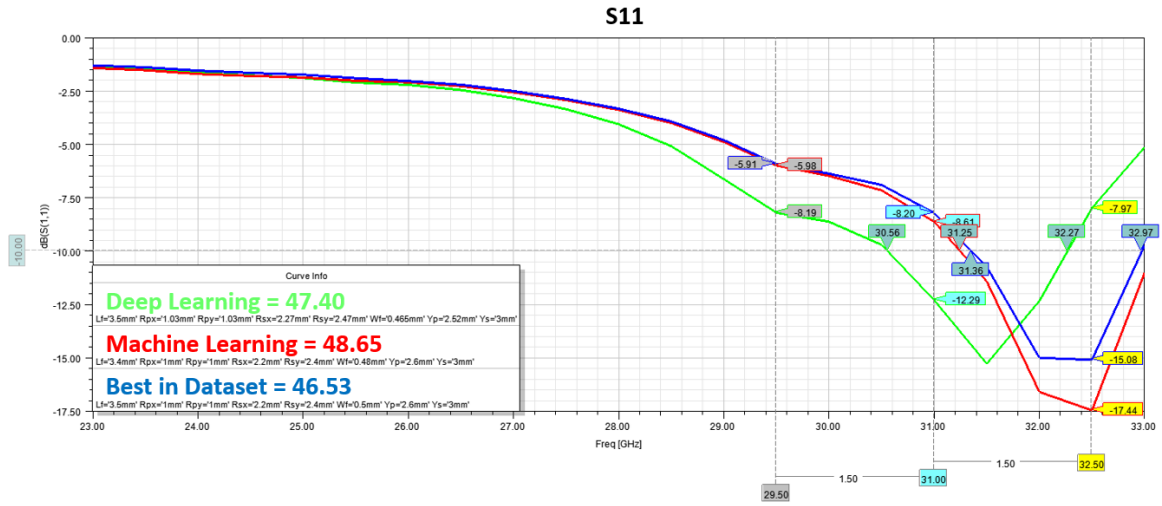

Figure 33: S11 of 31 GHz designs for machine learning, deep learning, and the best in dataset

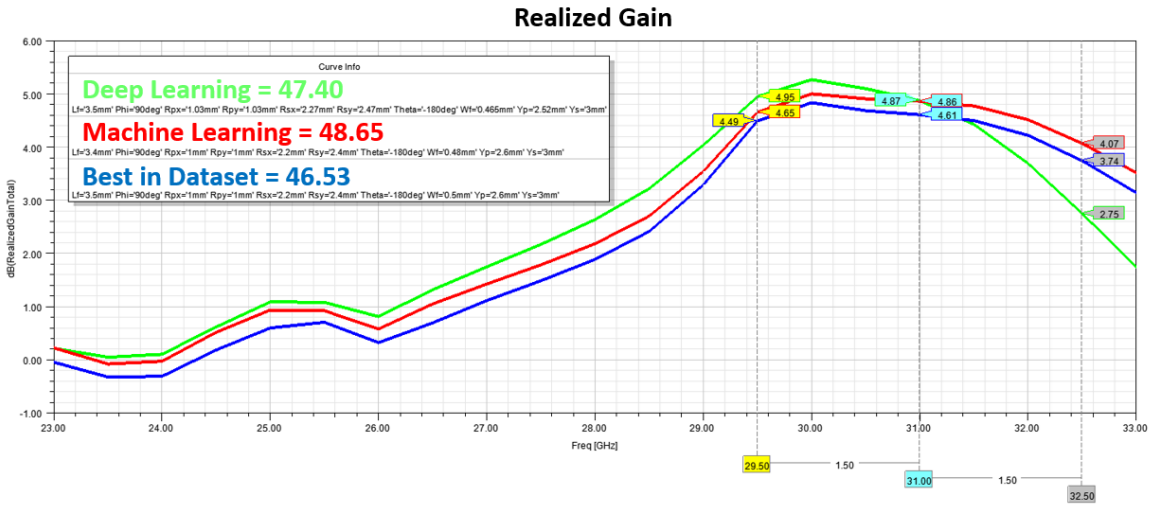

Figure 34: RG of 31 GHz designs for machine learning, deep learning, and the best in dataset

Final comparison of the scores with respect to machine learning tools and HFSS simulations is given Table 18. Both the machine learning and HFSS scores of traditional and best in the dataset for 28 GHz are very close to each other. The 28 GHz machine learning design's HFSS score was higher than the estimation score and the opposite is true for deep learning. Nevertheless, both scores of both designs were higher than the goal 53.92 score.

For 25 GHz and 31 GHz, points of comparison were chosen with respect to the best performing designs in the dataset. In both frequencies, designs were able to have 1 – 2

point higher score than the dataset design, which was also true for the designs of 28 GHz. Every score value for every design can be seen in Table 18.

FREQUENCY	METHOD	CALCULATION TIME (S)	ESTIMATED SCORE	HFSS SCORE
28 GHZ	Machine Learning	0.026	56.04	57.74
	Deep Learning	0.150	57.72	57.16
25 GHZ	Machine Learning	0.025	50.13	49.43
	Deep Learning	0.147	51.21	50.25
31 GHZ	Machine Learning	0.020	48.35	48.65
	Deep Learning	0.140	47.23	47.40

Table 18: Calculated scores of the designs with respect to machine learning estimations and HFSS simulation

8.3. Fabrication Results

After the fabrication of the antennae, S11 and gain values were compared to the best machine learning/ deep learning designs. Measurements were taken with respect to the reference antenna, so to find the actual gain, the relationship given below must be used:

$$DUT\ Measurement + (Reference\ Gain - Reference\ Measurement) + S11\ Correction + Conector\ Losses = Actual\ DUT\ Gain \quad (8.1)$$

After the measurement of S11 and calculations of the gains, measurement data were combined with simulation data. In Figure 35 and Figure 36, it can be seen that significant performance degradation is observed for both S11 and gain. A similar case was also observed for 28 GHz and 31 GHz designs. Even though some matching were observed

for 30 – 33 GHz in the 28 GHz design, lower performance was observed for fabricated antennae in general.

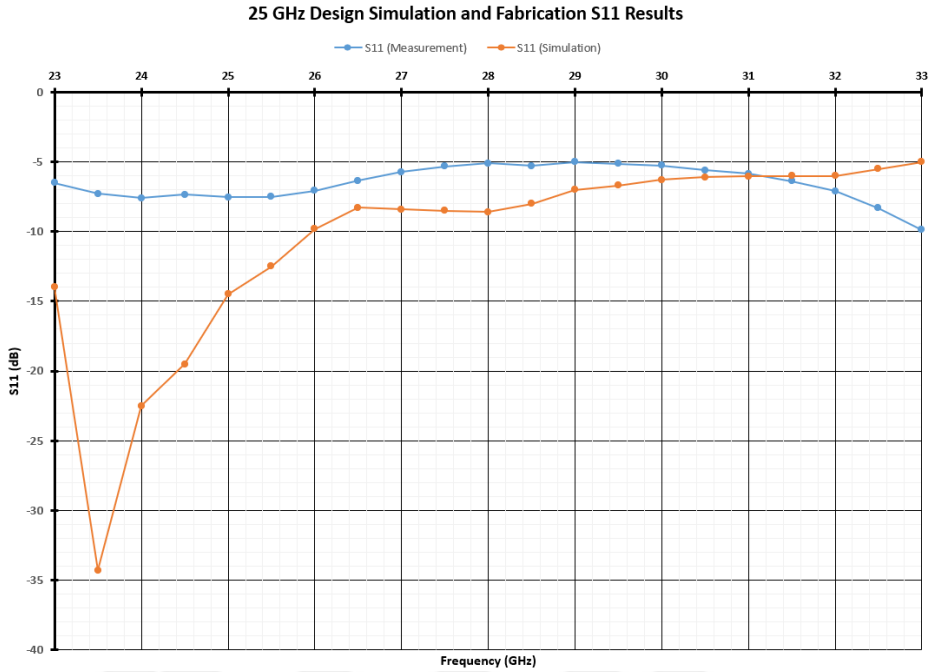

Figure 35: Fabrication and simulation S11 results of 25 GHz design

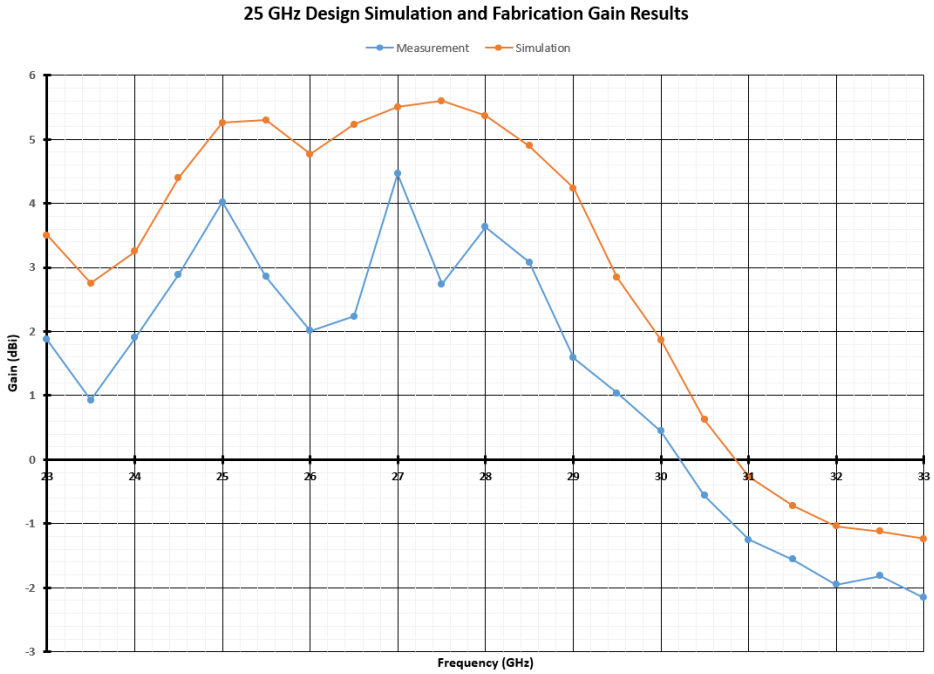

Figure 36: Fabrication and simulation gain results of 25 GHz design

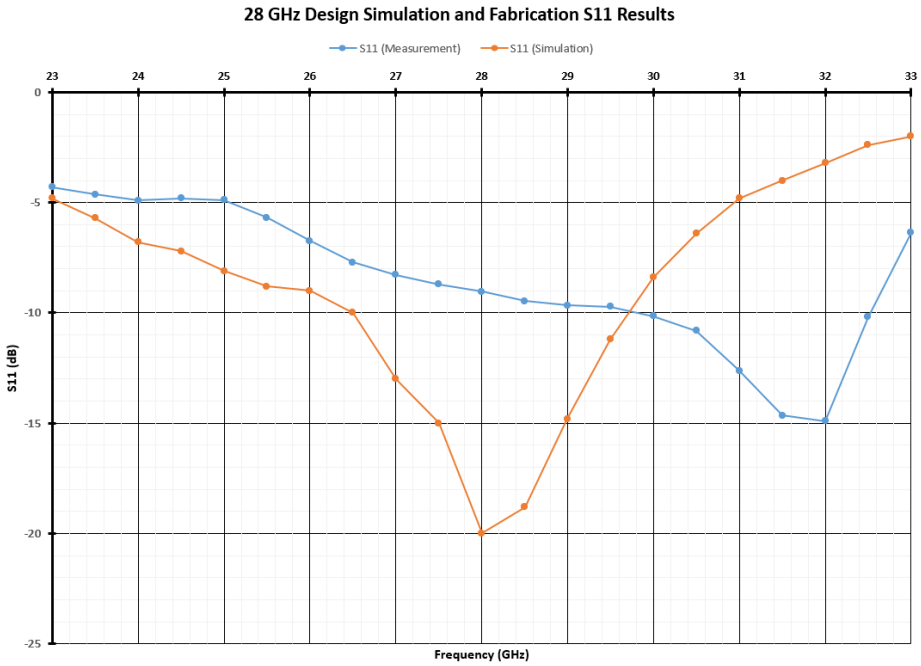

Figure 37: Fabrication and simulation S11 results of 28 GHz design

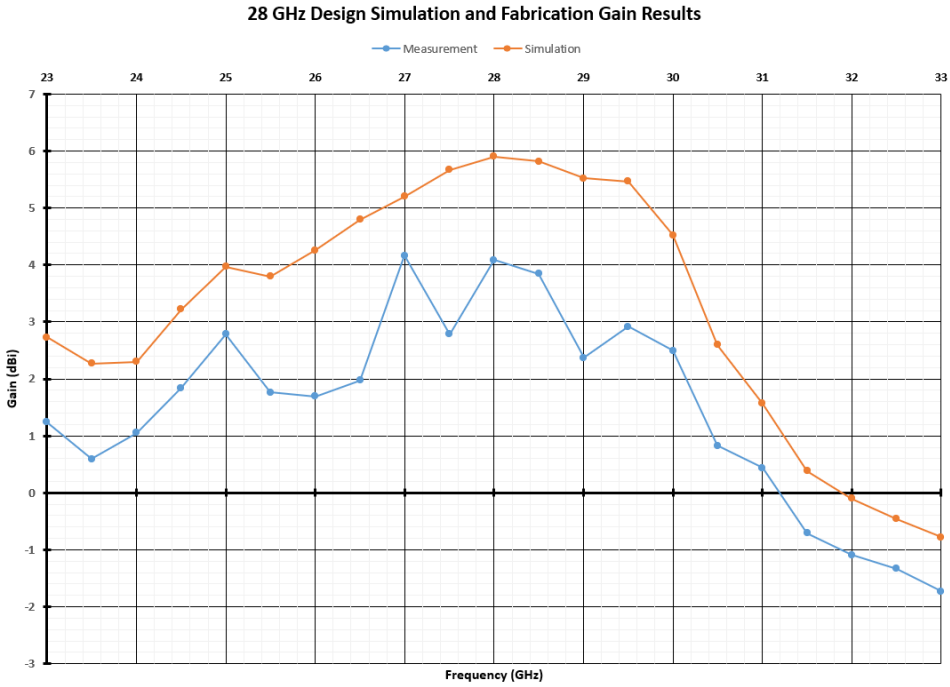

Figure 38: Fabrication and simulation gain results of 28 GHz design

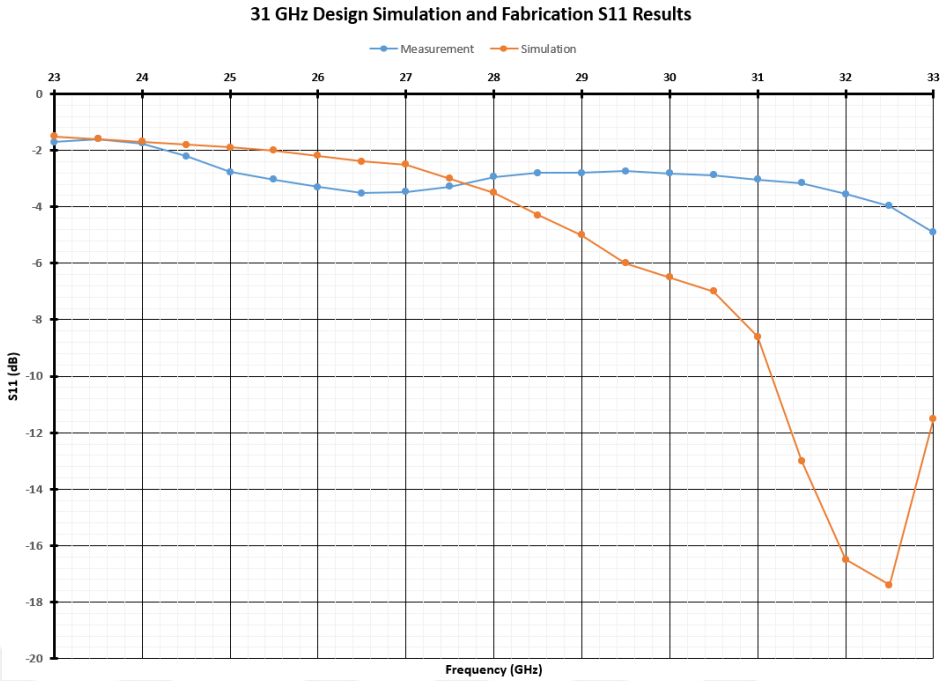

Figure 39: Fabrication and simulation S11 results of 31 GHz design

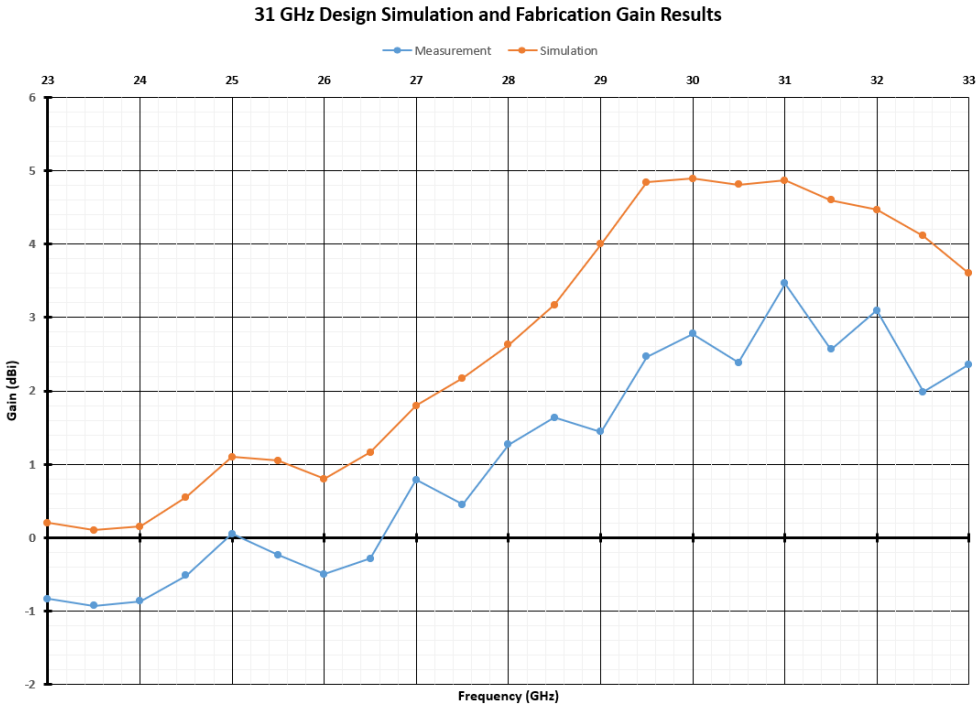

Figure 40: Fabrication and simulation gain results of 31 GHz design

CONCLUSION

In the beginning of the thesis, it was stated that the goal was to design a slot antenna for 5G n257 band using machine learning. This antenna had to be designed faster than the simulations done in HFSS and must have better results. End results proved that:

- Both neural networks and machine learning tools were able to design the antenna faster than the HFSS simulation. The expectation was set as a 10-fold increase in speed, but both machine learning and deep learning were able to surpass the expectations. Other works in the literature also pointed out the speed of these estimation tools, so these results were not a surprise.

- Both machine learning and deep learning designs had scores 1 – 2 points higher than the initial proposed antenna. Even though an increase was achieved there are some issues that must be underlined:

    - For the 28 GHz design, the traditionally designed antenna had similar performance compared to other works in the literature, so it is hard to comment on the increase observed with learning tools. The results were higher than the state of art, so it is hard to tell whether this design had the best performance possible or there is another better design which we don't know yet.

    - For the 25 GHz and 31 GHz designs, the degree of improvement was close to the improvement observed in 28 GHz with respect to the best designs in the dataset, but the score levels were not same. From the state of the art and the results observed from 28 GHz, it was known that scores around 55 are possible, which was not achieved by both the 25 GHz and 31 GHz

designs. Thus, it is clear to say that the improvement observed is limited by the dataset. If the frequency of interest includes low score designs, then the design generated by the learning tools will be lower compared to the other designs generated at other frequencies. Although this is a logical thing to observe, dependency on the dataset is a major flaw.

- The general behavior of the algorithms was also different from each other. In every frequency of design, machine learning results were slightly improved versions of the best designs found in the dataset. For deep learning, there was always a part which was way different than the best design in the dataset. For example, every design at 28 GHz was centered at 28 GHz, but deep learning design was centered at 29 GHz. The different behavior is clearer when the 25 GHz and 31 GHz designs were compared. In a way, designs generated by deep learning are more unique to an extent which also reasonable. For machine learning, random forest technique was used which was based on dividing dataspace into parts to make a prediction. Thus, the result found was closely related to dataspace. For deep learning, neural networks were used to create a multistep model with various activation conditions. Thus, the estimation was more dependent on the model than the dataspace. From this perspective, it can be said that deep learning has a higher potential to find better results, but computation time is a deterrent compared to machine learning.

To sum up the argument, it can be said that the set goals were achieved with some remarks, but this does not mean that every aspect of the proposed problem was covered. For example:

- All the work done in the thesis was done with respect to a single topology. If another topology was required, then the whole work done for traditional design and machine learning design had to restart. Even though it was far easier for machine learning to adapt because it is just a change of input and output size, it still requires generating a new dataset, which is time-consuming. A more general method, which can be applied to multiple topologies, can be the next step for the machine learning tools.

- Although machine learning tools are faster in general compared to HFSS, they are also suffering from complexity problems. For example, would the proposed method be feasible for a dataset which contains millions of data points? Unfortunately, testing this hypothesis also requires the generation of data, which is not feasible. This aspect may be investigated if the proposed methods are applied to another problem with more data available.

- The nature of the prediction algorithms depends on their hyperparameters and the number of configurations that can be tested is limitless. This thesis used the rule of thumbs and commonly used methods to tune hyperparameters, but there is always room for testing other setups.

For the results of the fabrication process, a separate section must be given. Due to the high frequency nature of the process, many parasitic effects can change the results. For this fabrication process, observed problems can be listed as:

- Tolerances. The designs were very sensitive to placement of radiating and reflector elements. Thus, any error in the placement directly affects the results.

- Feedline pin. The connector used for measurement feeds the antenna by pressing the pin to feedline with mechanical pressure. It is hard to say that this connection is reliable without any soldering.

- Connector screw placement. Connector screws were fixed with a small aperture under the screw holes. Unlike the CAD models given by the manufacturer, these apertures require a larger connector headroom, which was not the case. Direct connection with these apertures and the reflector layers made the floating ground a real ground, which directly changed the behavior of the antenna.

    - A larger headroom could have been given, but this would also change the performance of the antenna.

- Usage of reference antenna. It is important to note that the gain values were calculated with respect to a reference measurement, so any error in the reference measurement is also reflected in measurements done for this project.

Many other factors can be listed, but it has been proven that this topology was not suitable for simple fabrication even though it was advantageous for machine learning.

REFERENCES

[1] P. W. Futter and J. Soler, "Antenna design for 5g communications," in *2017 Sixth Asia-Pacific Conference on Antennas and Propagation (APCAP)*, Xi'an, 2017.

[2] G. Thirunavukkarasu and G. Murugesan, "A Comprehensive Survey on Air-Interfaces for 5G and beyond," *2019 10th International Conference on Computing, Communication and Networking Technologies (ICCCNT)*, pp. 1-7, 2019.

[3] C. Stocchi, N. Marchetti and N. R. Prasad, "Self-optimized radio resource management techniques for LTE-A local area deployments," 2011.

[4] T. Xu and I. Darwazeh, "Non-Orthogonal Frequency Division Multiple Access," in *2020 IEEE 91st Vehicular Technology Conference (VTC2020-Spring)*, Antwerp, 2020.

[5] I. Parvez, A. Rahmati, I. Guvenc, A. I. Sarwat and H. Dai, "A Survey on Low Latency Towards 5G: RAN, Core Network and Caching Solutions," *IEEE Communications Surveys & Tutorials (Volume: 20, Issue: 4, Fourthquarter 2018)*, pp. 3098 - 3130, 2018.

[6] Y. Huo, X. Dong and W. Xu, "5G Cellular User Equipment: From Theory to Practical Hardware Design," *IEEE Access* , vol. 5, pp. 13992 - 14010, 2017.

[7] H. T. Friis, "A Note on a Simple Transmission Formula," *Proceedings of the IRE* , pp. 254 - 256, 1946.

[8] M. S. Islam, F. Begum, A. U. Hani and M. A. Matin, "On the determination of penetration losses of microwave signals in different building materials," in *5th Brunei International Conference on Engineering and Technology (BICET 2014)*, Bandar Seri Begawan, 2014.

[9] Z. Pi and F. Khan, "An introduction to millimeter-wave mobile broadband systems," *IEEE Communications Magazine (Volume: 49, Issue: 6, June 2011)*, pp. 101 - 107, 2011.

[10] S. F. Jilani, Q. H. Abbasi and A. Alomainly, "Inkjet-Printed Millimetre-Wave PET-Based Flexible Antenna for 5G Wireless Applications," in *: 2018 IEEE MTT-S*

International Microwave Workshop Series on 5G Hardware and System Technologies, Dublin, 2018.

[11] J. Park, S. Y. Lee, Y. Kim, J. Lee and W. Hong, "Hybrid Antenna Module Concept for 28 GHz 5G Beamsteering Cellular Devices," in *2018 IEEE MTT-S International Microwave Workshop Series on 5G Hardware and System Technologies (IMWS-5G)*, Dublin, 2018.

[12] Z. Cendes, "The development of HFSS," in *2016 USNC-URSI Radio Science Meeting*, Fajardo, 2016.

[13] ANSYS, "Ansys INNOVATION Courses," [Online]. Available: https://courses.ansys.com/wp-content/uploads/2021/07/HFSS_3DLGS_2019R3_EN_LE03_Sol-1.pdf.

[14] G. Gampala and C. J. Reddy, "Fast and Intelligent Antenna Design Optimization using Machine Learning," in *2020 International Applied Computational Electromagnetics Society Symposium (ACES)*, Monterey, 2020.

[15] H. M. E. Misilmani and T. Naous, "Machine Learning in Antenna Design: An Overview on Machine Learning Concept and Algorithms," in *2019 International Conference on High Performance Computing & Simulation (HPCS)*, Dublin, 2019.

[16] E. Balevi and J. G. Andrews, "Online Antenna Tuning in Heterogeneous Cellular Networks With Deep Reinforcement Learning," *IEEE Transactions on Cognitive Communications and Networking*, 2019.

[17] "5G Frequency Bands," 2019. [Online]. Available: https://halberdbastion.com/technology/cellular/5g-nr/5g-frequency-bands.

[18] A. Zhao and F. Ai, "5G mm-Wave Antenna Array Based on T-Slot Antenna for Mobile Terminals," in *2018 IEEE Asia-Pacific Conference on Antennas and Propagation (APCAP)*, Auckland, 2018.

[19] M. S. Sharawi and M. Ikram, "Slot-based connected antenna arrays for 5G mobile terminals," in *2018 International Workshop on Antenna Technology (iWAT)*, Nanjing, 2018.

[20] T. Varum and J. N. Matos, "Compact Slot Antenna Array for 5G Communications," in *2019 IEEE International Symposium on Antennas and Propagation and USNC-URSI Radio Science Meeting*, Atlanta, 2019.

[21] M. M. M. Ali, O. Haraz, S. Alshebeili and A. R. Sebak, "Broadband printed slot antenna for the fifth generation (5G) mobile and wireless communications," in *2016 17th International Symposium on Antenna Technology and Applied Electromagnetics (ANTEM)*, Montreal, 2016.

[22] C. A. Balanis, Antenna Theory Analysis and Design, New York: John Wily & Sons, 1996.

[23] M. Morgan and S. Weinreb, "A millimeter-wave perpendicular coax-to-microstrip transition," in *2002 IEEE MTT-S International Microwave Symposium Digest (Cat. No.02CH37278)*, IEEE, 2002.

[24] M. K. Khattak, S. Kahng, M. S. Khattak and A. Rehman, "A low profile, wideband and high gain beam-steering antenna for 5G mobile communication," in *2017 IEEE International Symposium on Antennas and Propagation & USNC/URSI National Radio Science Meeting*, San Diego, 2017.

[25] H. Yon, M. T. Ali, M. A. Aris and B. Baharom, "A New Model Microstrip Antenna like Microphone Structure for 5G Application," in *2018 IEEE International RF and Microwave Conference (RFM)*, Penang, 2018.

[26] N. Ojaroudiparchin, M. Shen, S. Zhang and G. F. Pedersen, "A Switchable 3-D-Coverage-Phased Array Antenna Package for 5G Mobile Terminals," *IEEE Antennas and Wireless Propagation Letters ,* pp. 1747 - 1750, 2016.

[27] Z. Ahmed, P. McEvoy and M. J. Ammann, "Comparison of Grid Array and Microstrip Patch Array Antennas at 28 GHz," in *2018 IEEE MTT-S International Microwave Workshop Series on 5G Hardware and System Technologies (IMWS-5G)*, Dublin, 2018.

[28] S. Rong and Z. Bao-wen, "The research of regression model in machine learning field," in *MATEC Web of Conferences*, 2018.

[29] J. Brownlee, "Machine Learning Mastery," 27 March 2020. [Online]. Available: https://machinelearningmastery.com/multi-output-regression-models-with-python/.

[30] A. Abel and B. S. Bernanke, Macroeconomics, Pearson Addison Wesley, 2005.

[31] T. Hastie, R. Tibshirani and J. Friedman, The Elements of Statistical Learning: Data Mining, Inference, and Prediction, 2001.

[32] A. Navada, A. N. Ansari, S. Patil and B. A. Sonkamble, "Overview of use of decision tree algorithms in machine learning," in *2011 IEEE Control and System Graduate Research Colloquium*, Shah Alam, 2011.

[33] "K-Neighbors Classifier," Scikit Learn, [Online]. Available: https://scikit-learn.org/stable/modules/generated/sklearn.neighbors.KNeighborsClassifier.html. [Accessed 17 February 2022].

[34] "Decision Tree Regressor," Scikit Learn, [Online]. Available: https://scikit-learn.org/stable/modules/generated/sklearn.tree.DecisionTreeRegressor.html. [Accessed 18 February 2022].

[35] "Random Forest Classifer," Scikit Learn, [Online]. Available: https://scikit-learn.org/stable/modules/generated/sklearn.ensemble.RandomForestClassifier.html. [Accessed 16 February 2022].

[36] E. Alpaydin, "Neural Networks and Deep Learning," in *Machine Learning: The New AI*, MIT Press, 2016, pp. 85 - 109.